Risk Evaluation for combined flood seismic hazards for strategic structures with water lifting plants

Indexes of exposure combined flood seismic risk exposure for IT pilot site

---

Final Version of 31/03/2022

Deliverables Number D.4.1.3. - D.4.2.3 – D.4.2.4

European Regional Development Fund

www.italy-croatia.eu/pmo-gate

Project Acronym	PMO-GATE
Project ID Number	10046122
Project Title	Preventing, Managing and Overcoming natural-hazards risk to mitiGATE economic and social impact
Priority Axis	2: Safety and Resilience
Specific objective	2.2: Increase the safety of the Programme area from natural and man-made disaster
Work Package Number	4
Work Package Title	Assessment of multi-hazard exposure in coastal and urban areas
Activity Number	4.1, 4.2
Activity Title	ACTIVITY 4.1 Assessment of combined flood-seismic hazards ACTIVITY 4.2 Assessment of combined seismic-flood-(meteo tsunami) hazards coast floods
Partner in Charge	UNIFE
Partners involved	FGAG, MUNFE
Status	Final
Distribution	Public

Table of content

PART A: Risk Evaluation for combined flood seismic hazards for strategic structures with water lifting plants: the use of a Machine Learning algorithm

PART B: Indexes of exposure combined flood seismic risk exposure for IT pilot site: the use of the Multi Criteria Decision Making method PROMETHEE

The present deliverable gathers the results obtained by applying two different advanced multirisk methodologies for the evaluation of combined risks of hydraulic and seismic type. The two methodologies are described hereafter in part A and part B, respectively. We have decided to report here both the risk analysis and the indexes obtained as they are closely related. Any multirisk methodology cannot deal with local data but requires regional data or at least data relating to a sufficiently vast area to be able to define risk indexes. Therefore, the structural scale was not considered, and the regional scale was instead taken into account.

A. Premise on the use of AI methods for multirisk assessment

Social vulnerability is deeply affected by the increase in hazardous events such as earthquakes and floods. Such hazards have the potential to greatly affect communities, including in developed countries. Governments and stakeholders must adopt suitable risk reduction strategies. This study is aimed at proposing a qualitative multi-hazard risk analysis methodology in the case of combined seismic and flood risk using PROMETHEE, a Multiple-Criteria Decision Analysis technique. The present case study is a multi-hazard risk assessment of the Ferrara province (Italy). The proposed approach is an original and flexible methodology to qualitatively prioritize urban centers affected by multi-hazard risks at the regional scale. It delivers a useful tool to stakeholders involved in the processes of hazard management and disaster mitigation.

Furthermore, this study is aimed at proposing a sound qualitative multi-hazard risk analysis methodology for the assessment of combined seismic and hydraulic risk at the regional scale, which can assist governments and stakeholders in decision making and prioritization of interventions. The method is based on the use of machine learning techniques to aggregate large datasets made of many variables different in nature each of which carries information related to specific risk components and clusterize observations. The framework is applied to the case study of the Emilia Romagna region, for which the different municipalities are grouped into four homogeneous clusters ranked in terms of relative levels of combined risk. The proposed approach proves to be robust and delivers a very useful tool for hazard management and disaster mitigation, particularly for multi-hazard modelling at the regional scale.

A.1. Introduction

The frequency of natural extreme events is increasing worldwide [1–9], and human activities often interact with devastating effects, affecting people and natural environments, and producing great economic losses, especially in developing countries. On the other hand, in some developed countries, disasters have been decreasing since the beginning of the 20th century [3,4]. Understanding risk involving vast inhabited areas is, therefore, paramount, particularly when assessing potential losses produced by a combination of multiple hazards, which are defined as the probability of occurrence in a specified period of a potentially damaging event of a given magnitude on a given area [5]. In fact, total risk is a measure of the expected human (casualties and injuries) and economic (damage to property and activity disruption) losses due to a particular adverse natural phenomenon. Such a measure is conceptually assumed as the product of hazard, vulnerability, and exposure instances [6]. Exposure of people to the consequences of extreme natural phenomena could be reduced if predictive models based on new approaches and deeper knowledge of effective factors were employed [7].

Many areas on Earth are subjected to the effects of coexisting multiple hazards, among which floods and earthquakes are some of the most widespread [8,9] and even if it is well established

that inhabited environments are affected by multiple hazardous processes, most studies focus on a single hazard [10]. However, hazards usually interact with each other and contribute to the overall risk in a complex way. For this reason, the development of multi-hazard risk assessment approaches is of first importance [11] and multi-hazard mapping is receiving increasing attention [12,13]. In particular, Schmidt et al. proposed a multi-hazard risk assessment methodology in New Zealand, devising an adaptable computational tool allowing its users to input the natural phenomena of interest [11]. Still, relatively scarce are the studies exploiting machine learning techniques to assess multi-hazard risks [14–16], albeit machine learning is especially useful when dealing with the huge amount of data encountered in risk analysis, particularly at the regional scale.

In this study, machine learning is used to construct a risk assessment framework in which the combined effects of two major natural events (flood and earthquakes) are analyzed for the Emilia Romagna test region (Italy). A large input dataset containing, for each municipality of the test region, a wide number of quantitative variables related to hazard, exposure, and vulnerability instances for both flood and earthquake hazards is adopted. Then, the number of variables is suitably reduced by means of Principal Component Analysis (PCA) [17–19], and the municipalities are subsequently grouped into four approximately risk-wise homogeneous clusters using a K-means clustering algorithm [20,21]. Finally, a qualitative overall risk level is assigned to each cluster. The proposed methodology represents a robust tool for the qualitative multi-hazard risk assessment at the regional scale, which enables suitable extraction of risk-related information from a large input dataset and provides a useful instrument that assists stakeholders in decision-making processes, especially with respect to intervention prioritization.

A.2. Materials and Methods

The proposed multi-hazard risk assessment approach is based on the analysis of available data using logical, mathematical, and statistical tools. It was applied to the Emilia Romagna region, which is located in the Northern part of Italy. Our analysis focused on seismic and hydraulic risks associated with this territory. A map of the seismic classification of municipalities in Emilia is shown in Figure 1. A hot-spot of hydraulic risk in Emilia Romagna, Ferrara possesses an altimetry below the sea level over a large part of its territory, as illustrated in Figure 2.

To evaluate the overall combined risk for the different municipalities in the test region, several intermediate steps were necessary. At first, the reliability of the method was tested on a smaller data sample given by the municipalities in the Province of Ferrara (Italy), then on a slightly larger one, considering municipalities from other provinces in the test region, and then, finally, expanding the data sample to each municipality of the Emilia Romagna region. This type of approach improved control on both the algorithm and its calibration, as well as the initial dataset,

leading to a significant reduction in terms of computational time. In what follows, we omit the description of the intermediate steps and directly present the analysis for the whole test region.

2.1. Dataset

Choosing the correct amount of data is paramount. The data employed for our analysis have been obtained from the Italian National Institute of Statistics (ISTAT) database, which was used in 2018 by the Italian Superior Institute for Environmental Protection and Research (ISPRA) to produce seismic, hydrogeological, volcanic, and social vulnerability hazard maps for the entire Italian peninsula as shown in the report by Trigila et al. [22]. These maps constitute a fundamental tool of support to national risk mitigation policies, allowing the identification of intervention priorities, the allocation of funds, and the planning of soil protection interventions.

The input dataset was organized as a matrix in which the rows corresponded to each of the 331 municipalities of the Emilia-Romagna region and the columns corresponded to quantitative variables associated with different aspects of seismic and flood risk. Hence, we had 331 rows or observations and hundreds of columns or variables. For instance, we adopted as variables the number of buildings sharing certain features (such as building material, the period of construction, or the state of conservation), superficial extension, number of inhabitants, population density, seismic peak ground acceleration, etc. Overall, all the variables can be grouped into three macro-categories: variables related to vulnerability instances, variables related to exposure instances, and variables related to hazard instances for both seismic and hydraulic risks.

Since hydraulic risk, as a combination of hydraulic vulnerability, exposure, and hazard, has previously been evaluated for each observation by the Italian National Institute of Geophysics and Vulcanology (INGV), it was represented in the proposed analysis as a unique variable, which condensed all the variables related to hydraulic risk.

The relative importance between some variables and the relation among them is quantified by means of the PCA method, which will be described in the next subsections.

For instance, some of the crucial variables were identified as follows:

- agMAX_50: maximum value of the peak ground acceleration about the grid data point;
- DENSPOP: Population density (n. of inhabitants/kmq);
- E1-E31: Type of Buildings (e.g., residential, masonry, and state of conservation);
- IDR_AreaP1/P2/P3: Hydraulic risk surface, respectively, low/medium/high;
- IDR_PopP1/P2/P3: Population living in, respectively, low/medium/high hydraulic risk surface.

An extensive table reporting the explanations of all acronyms associated with the relevant variables is reported in Appendix A.

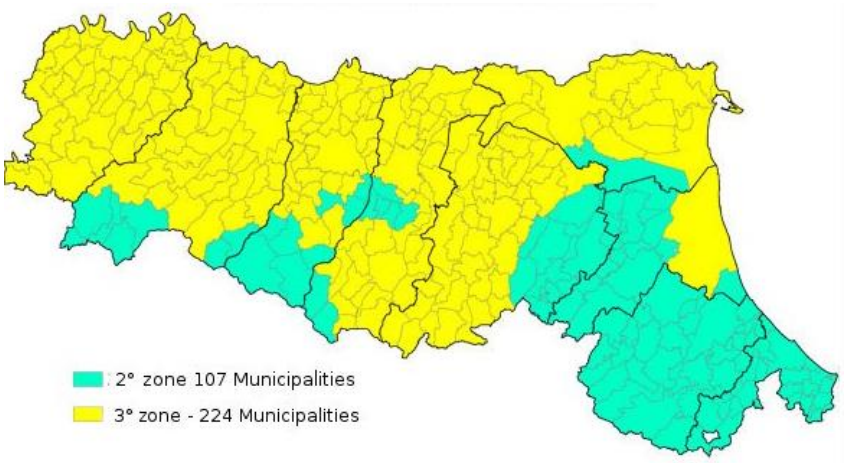

Figure 1. Seismic classification of municipalities in Emilia (https://ambiente.regione.emilia-romagna.it/en/geologia/seismic-risk/seismic-classification, accessed 15/10/2021).

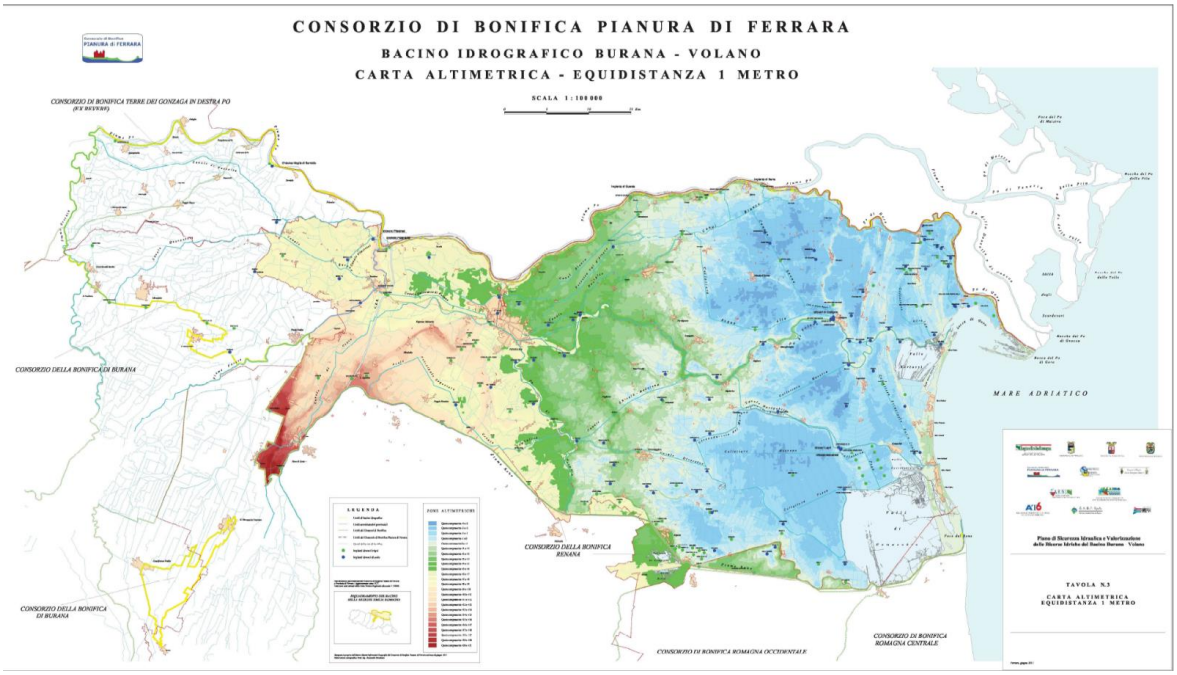

Figure 2. Ferrara territory altimetry (The map can be downloaded from https://www.bonificaferrara.it and has been released from "Consorzio di Bonifica Pianura di Ferrara"; accessed 15/10/2021).

A.2.2. Initial Exploratory Analysis

Exploratory analysis is a typical analytical approach in statistics that is suitable for defining and synthesizing the main characteristics of a group of data. This type of approach enables preliminarily evaluating, searching, and finally, analyzing possible notable patterns within the data, in a phase where possible interactions among variables are not known yet. Again, graphics techniques for data visualization are quite useful in this step, producing diagrams such as box plots, scatter plots, histograms, etc. More analytical techniques, such as PCA, are very useful. The whole proposed analysis has been implemented and performed in a MATLAB computing environment [23].

A.2.2.1. Standardization

The first step of the exploratory analysis is data standardization. As usual [15,16], the metric of standard deviation was adopted to test the machine learning model's accuracy and to measure confidence in the obtained statistical conclusions. This allows us to compare variable data with different units of measure, scaling all the variables such that each scaled variable will have mean value equal to 0 and standard deviation equal to 1, referred to the data distribution for each variable. To attain this outcome, for each variable χ of the dataset, mean μ and the standard deviation σ have been calculated. Then the z-score formula has been applied:

$$z = \frac{x - \mu}{\sigma}. \tag{1}$$

A.2.2.2. PCA

Once the entire dataset was standardized, PCA was applied. One of the main targets of PCA is to reduce the dimensionality of the initial dataset without losing the amount of information belonging to it. A dimensionality reduction technique is a process that takes advantage of linear algebraic operations to convert an *n*-dimensional dataset to an *n-k* dimensional one. Clearly, this transformation comes at the cost of a certain loss of information, but it also gives the benefit of being able to graphically visualize the data, while keeping good accuracy.

The idea behind PCA is to find the best subspace, which explicates the highest possible variance in the dataset. Using linear transformations, starting from an initial standardized matrix in the n-dimensional space, changes in variables are carried out that makes possible to identify observations in the space generated from the principal components, which have the particularity to catch the maximum possible variance of the initial dataset, thus reducing the loss of information.

Given *p* random standardized variables $X_1, X_2, \ldots, X_p$, collected into the matrix X, the analysis allows determining $k < p$ variables $Y_1, Y_2, \ldots, Y_k$, each of them a linear combination of the *p* starting

variables, having maximum variance. To find Y_i, also known as the *i*-th principal component, we need to find the vector V_i such that

$$Y_i = \tilde{X}V_i \tag{2}$$

by maximizing the variance relative to the first principal component. In other words, vectors V_i are the eigenvectors of the covariance matrix C of $\tilde{X}$, i.e., the $n \times p$ matrix whose generic element C_{hk} is equal to $COV(\tilde{X}_h, \tilde{X}_k)$.

The *j*-th element of Y_i represents the *score* of the *i*-th principal component for *j*-th statistical unit. The *j*-th element of V_i represents the *weight* that the *j*-th variable $\tilde{X}_j$ has in the definition of the *i*-th principal component. Vectors V_i can be collected as columns in the matrix of weights V.

Lastly, axis rotations are applied, which mean a change of position of the dimensions obtained during the factor's extraction phase, keeping the initial variance fixed as much as possible. The axis can be rigidly rotated (orthogonal rotation) or interrelated (oblique rotation). The result is a new matrix of rotated factors.

Once the dimension of the dataset has been reduced, it is possible to plot the observations in the new space generated by the principal components, space where the coordinates of the observations have undergone linear transformation, in accordance with the variables as mentioned before.

The scatter plot represented in Figure 3, depicts the observations after variable reduction. One can notice the presence of elements defined as outliers, i.e., abnormal values, far from the average observations. These disturbing elements could generate unbalanced compensations inside the analytical model, and that is why they will be handled with care, modifying the algorithm's settings whenever possible or, in extreme cases, removed from the dataset. In this case, the outliers were almost all the administrative centers of Emilia-Romagna region, far away, in terms of the quantitative variables, from the rest of the observations.

It is a good rule to consider the principal components that catch at least 80% of the variance of the starting dataset. The more the considered variables, the higher the number of principal components necessary to reach that quote. Whenever the amount of variance reached is not sufficient, an additional reduction in variables is performed by iterating the process.

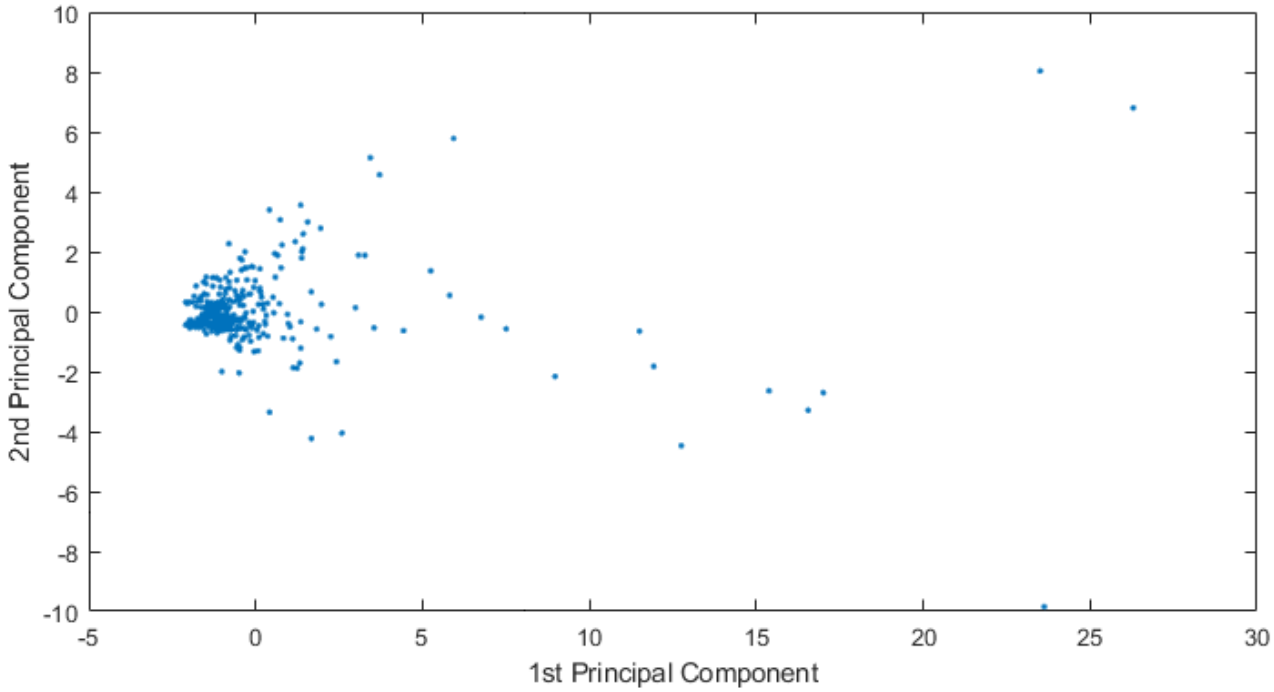

Figure 3. Observations scatter plot which depicts the observations after variable reduction.

One of PCA's main purposes is to delete the noise due to non-useful data, which is evaluated in terms of how much information and how much variance they carry inside the dataset. Figure 4 represents variance for each principal component before variable reduction. Loading plots have been generated as histograms representing the weight of the variables transformed after the PCA and are reported in Figures 5 and 6. The variables reported along the abscissa have been selected among all the available data for being the most meaningful as per the multi-risk evaluation. For instance, AGMAX_50 denotes the maximum ground acceleration (fiftieth percentile) calculated on a grid with a 0.02° step, with the maximum and minimum of the values of the grid points falling within the municipal area. IDR_POPP3 indicates the resident population at risk in areas with high hydraulic hazard (P3). From Figures 5 and 6, the variables with the highest coefficients have been extrapolated, the higher the coefficient of the variable, the higher the weight of the variable on the principal component. Along the first principal component, the difference between observations will be led by the different values referred to the variables with highest coefficient in the histogram depicted in Figure 5.

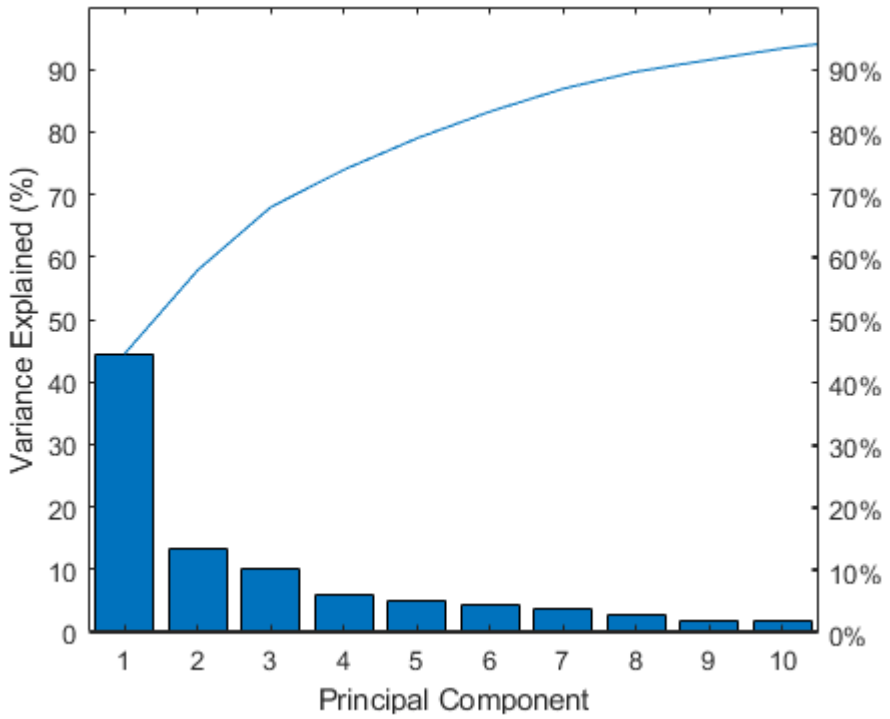

Figure 4. Variance for each principal component before variable reduction.

We chose to assess the weight of the coefficient of the variables referring to the first two principal components only, because they explicated more than 70% of the variance and are the most significant of the combined risk assessment. Figure 7 depicts the variance explicated by the first 10 principal components after the PCA.

Fundamental to the visualization of both observations and the relation between the variables is the biplot in Figure 8.

This plot allows catching at an early stage any pattern within the dataset, such as the separation between observations and deep relation among variables. In general:

the projection of the values on each principal component shows how much weight those values have on that principal component;

when two vectors are close, in terms of angle, the two represented variables have a positive correlation;

if two vectors create a 90 angle, the respective variables are not correlated;

when they diverge and create an angle of almost 180, they are negatively correlated.

Outliers differ from the other observations in terms of vulnerability and the population at hydraulic risk. It is reasonable because, remembering the outliers are the provincial administrative centers, they present higher values in terms of population and built environment. Moreover, along the vertical axis the observations differ in terms of seismic hazard and exposition.

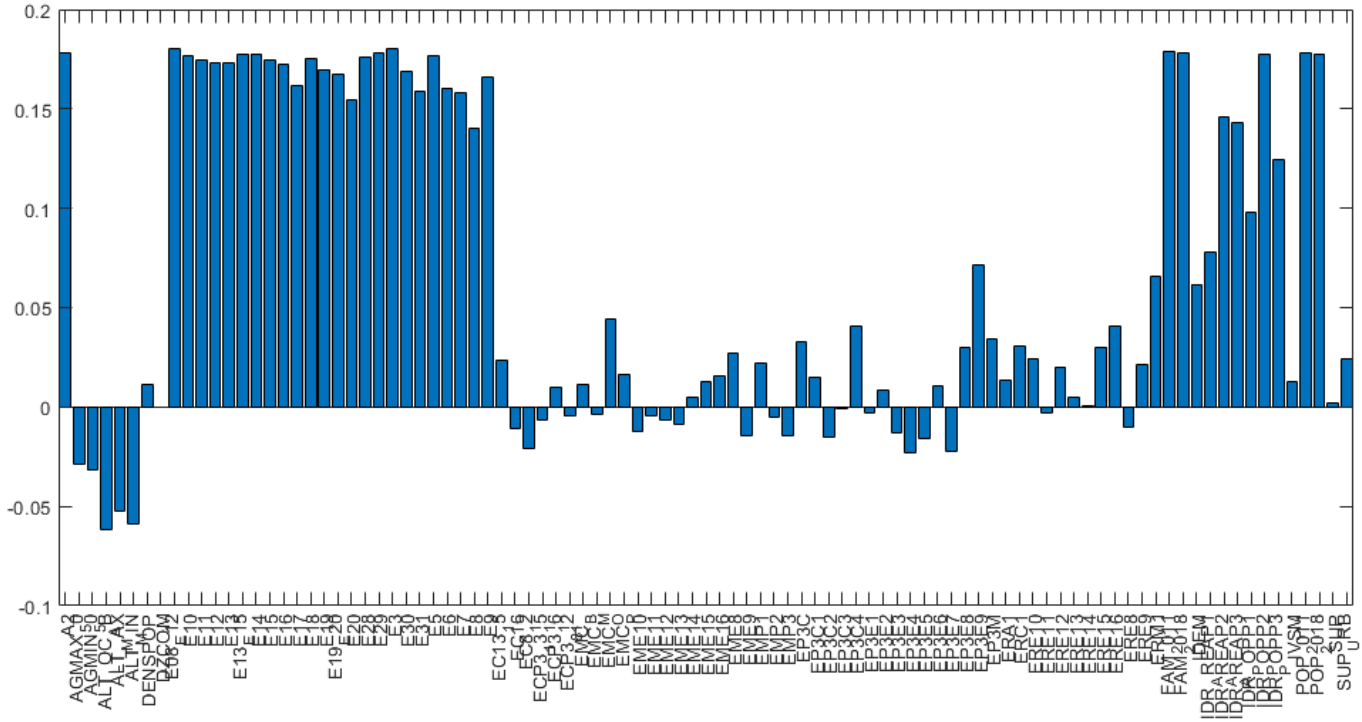

Figure 5. Loading plot of the variable coefficients along the first principal component (see Appendix A for an explanation of the acronyms).

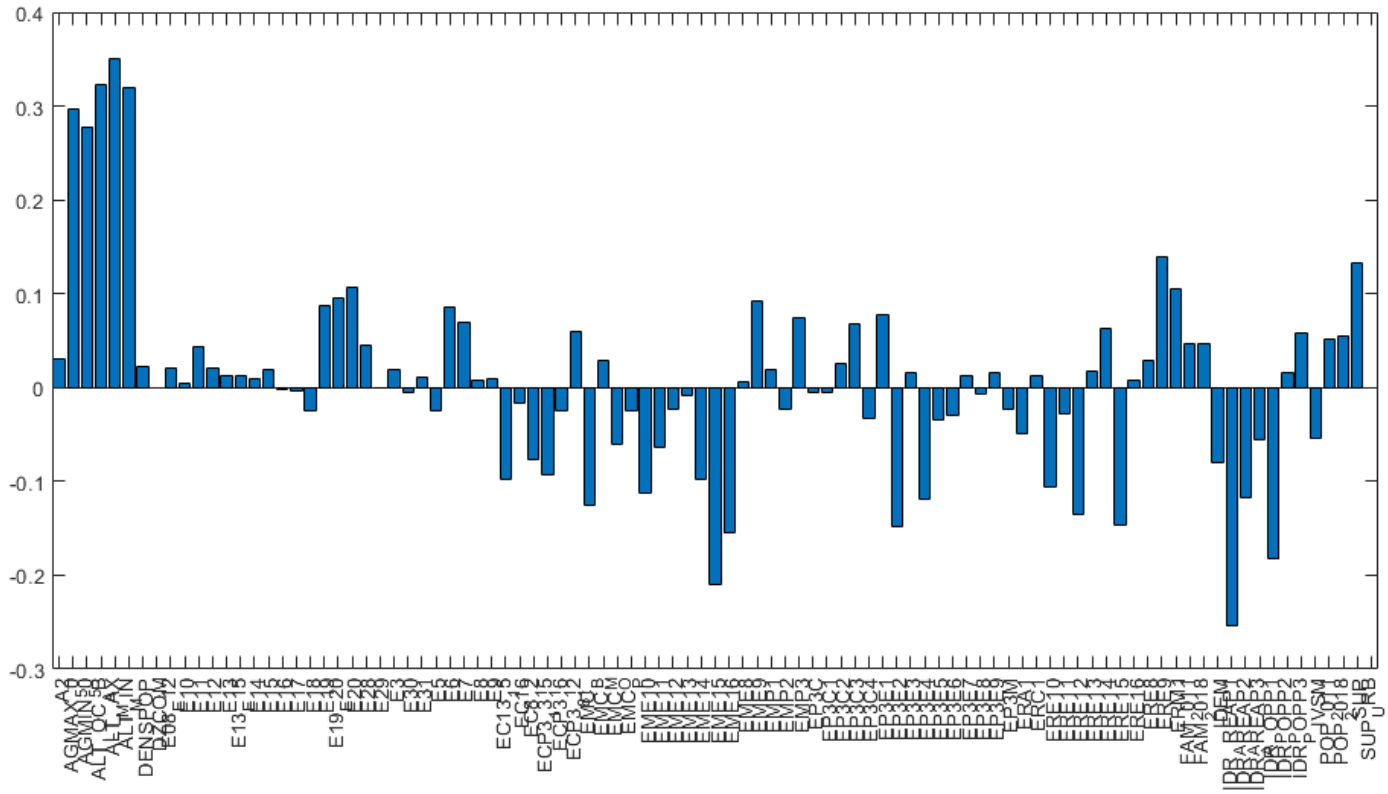

Figure 6. Loading plot of the variable coefficients along the second principal component (see Appendix A for an explanation of the acronyms).

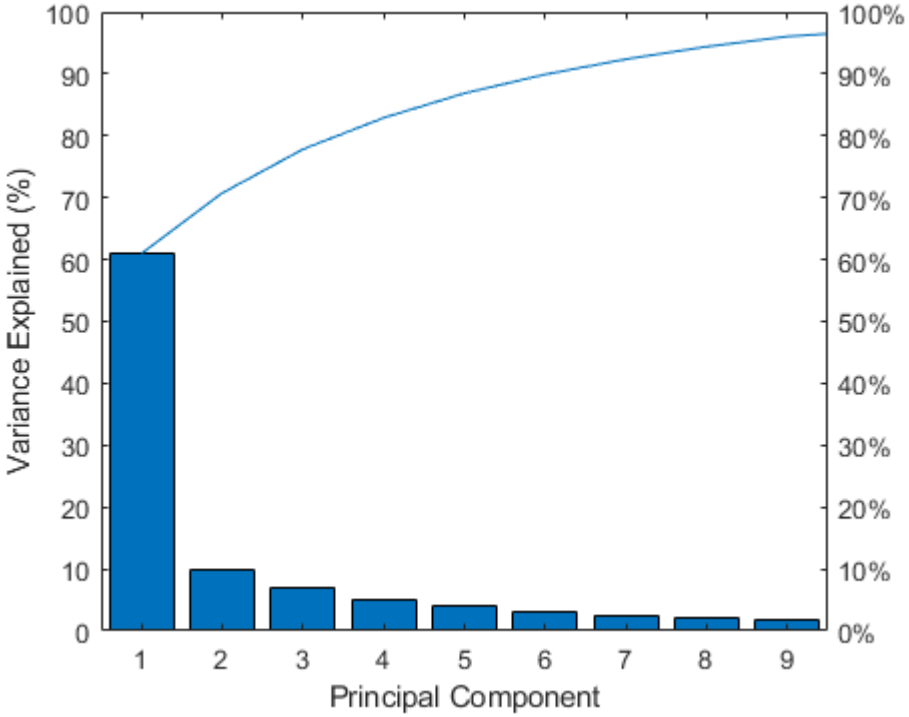

Figure 7. Variance of the first 10 principal components after variable reduction.

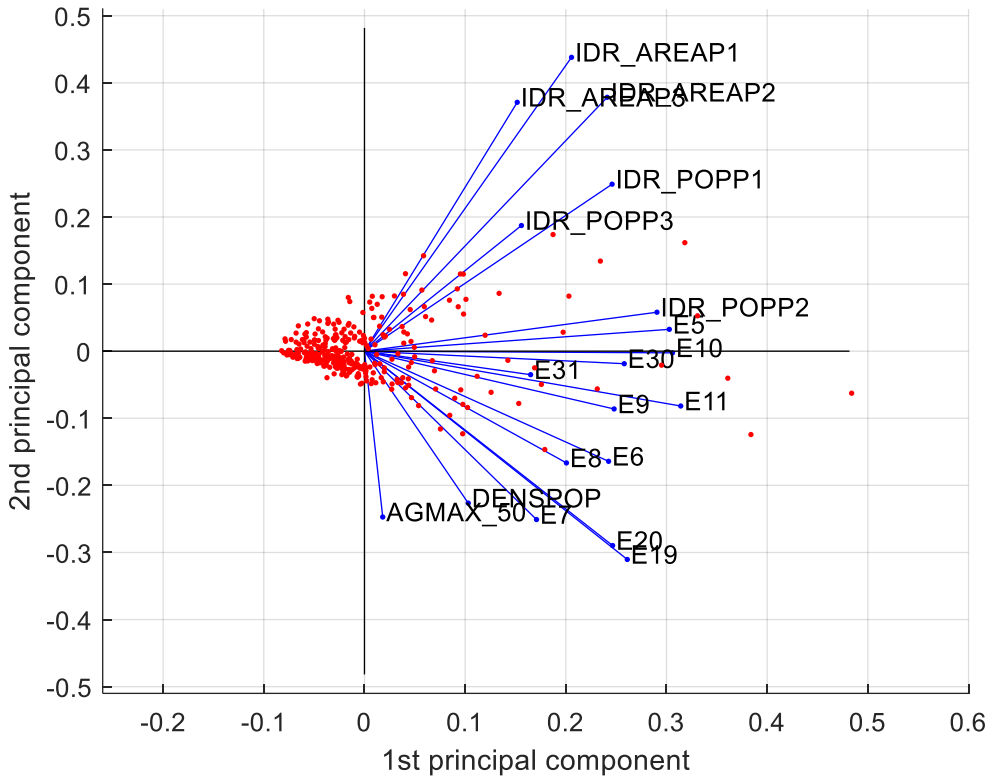

Figure 8. Biplot along the first two principal components.

Moreover, vulnerability and exposure to hydraulic risk variables are quite correlated and differentiate the observations along the horizontal axis, whereas seismic hazard and exposition variables are not correlated with the variables representing surfaces at hydraulic risk. These remarks will come in handy later, at a post-clustering stage, a level of multi-risk will be attributed to each cluster.

A.2.3. K-Means Clustering Algorithm

The PCA allowed us to reduce the dimensionality of the dataset and plot the observations, i.e., the municipalities of the Emilia Romagna region, in the new sub-space identified by the principal components, while retaining the majority of information, which identified the observations in the initial n-dimensional space before the linear transformations.

To suitably group the observations according to homogeneous levels of overall risk, we used an unsupervised machine learning algorithm, known as *k-means clustering*.

In general, cluster analysis is a technique to group data where the main purpose is to gather observations according to the features selected by the user. The analysis allows splitting a set of

observations into clusters according to similar or non-similar features. Cluster analysis does not require knowing the classes in advance, as in the case of supervised algorithms.

In the k-means clustering algorithm, we assumed N observations $x_1, x_2, \ldots, x_n$ and partitioned them into k clusters, each defined by a centroid $c_1, c_2, \ldots, c_k$. We assigned the x_i observation to the cluster, such that the distance among the observation and the cluster center was minimum.

The algorithm began by randomly choosing *k* centroids. After measuring the distance of each observation to each centroid, the observation was assigned to the closest cluster. Then, centroids were updated, as the average of the observations in each centroid. The procedure was repeated iteratively, each time minimizing the distance between observation and centroid.

Different choices for such distance function are possible and readily available in many scientific computing software packages such as MATLAB: the squared Euclidean distance, one minus the cosine of the included angle between points (treated as vectors), or one minus the sample correlation between points (treated as sequences of values).

In particular, the squared Euclidean metric does not allow keeping the outlier in the dataset because of the square of the distance. By doing so, the algorithm will place a specific cluster just for the outlier, influenced by its distance from the other observations. Later, we will propose a comparison among the distances in terms of the quality of clustering.

To legitimate the clusterization carried out with the k-means algorithm, the *silhouette method* was employed. The technique provided a succinct graphical representation of how well each observation has been classified. The silhouette value is a measure of how similar an object is to its own cluster (cohesion) compared to other clusters (separation). The silhouette ranges from −1 to +1, where a high value indicates that the object is well matched to its own cluster and poorly matched to neighboring clusters. If most objects have a high value, then the clustering configuration is appropriate. If many points have a low or negative value, then the clustering configuration may have too many or too few clusters. The silhouette can be calculated with any distance metric, such as the Euclidean distance or the so-called Manhattan distance.

To decide which metrics to adopt, a comparison based on the silhouette of each method was performed (see Figure 9). Correlation metrics appear to be the most reliable, whereas the squared Euclidean would be as good if it were not for the outliers.

A four clusters grouping was chosen for the proposed analysis. Figure 10 represents the final clusterization of Emilia-Romagna municipalities. Cluster evaluation was conducted considering the weight and the distribution of the variables. All the outliers belonged to cluster 4, which was developed both on the horizontal axis, led by seismic vulnerability and hydraulic risk variables, and slightly on the vertical one, led by seismic hazard and by hydraulic risk variables. The great majority

of the municipalities presented similar quantitative values of variables, in particular, those belonging to clusters 2 and 3. Silhouette values relative to this clusterization were good, reinforcing the reliability of the method proposed.

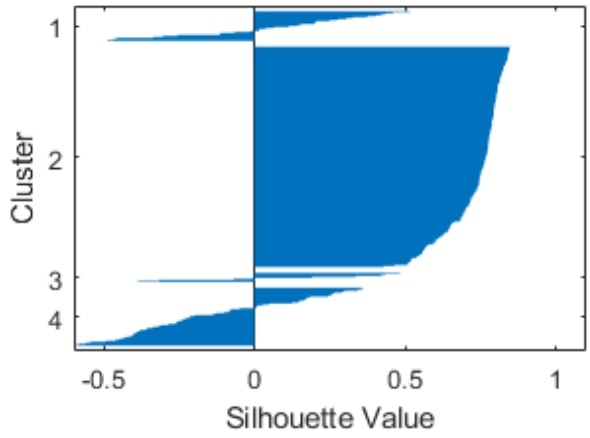

(**a**)

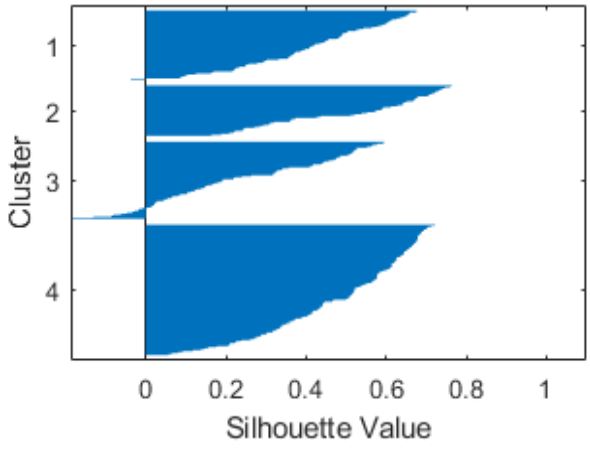

(**b**)

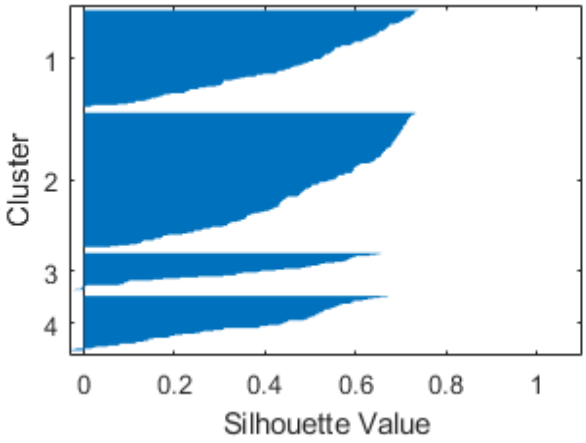

(c)

Figure 9. Silhouette for different metrics: squared Eculidean (a), cosine (b), and correlation (c).

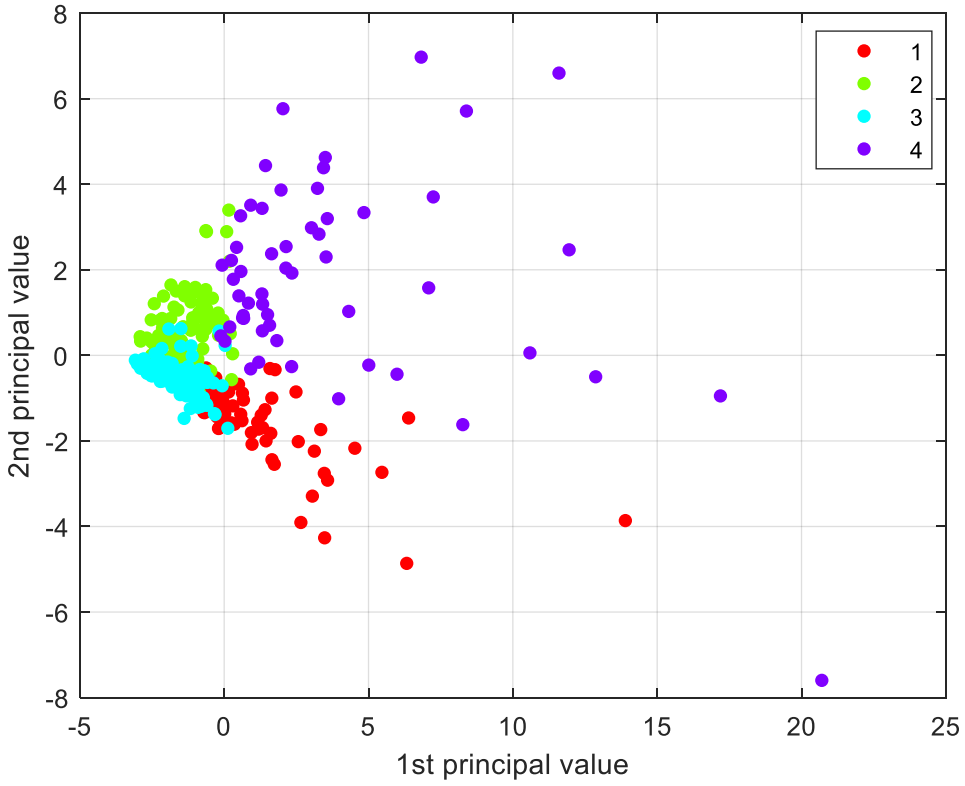

Figure 10. Grouping of the Emilia Romagna municipalities into four clusters.

A.3. Results

In this section, we show how to assign to each observation and, more generally, to each cluster, a label which identifies the associated level of overall risk.

3.1. Variables Label Assignment

First, we set intervals in an objective way, in order to suitably define labels for the variables. To this aim, we set interval extremals in correspondence of quartile percentages Q1, Q2, and Q3 as indicated in Table 1.

Table 1. Labels and intervals for cluster definition.

Intervals	**Label**
first element: Q1	Low
Q1: Q2	Medium-to-low
Q2: Q3	Medium-to-high
Q3: last element	High

The chosen labels referred, respectively, to the presence of low, medium-to-low, medium-to-high and high amounts regarding that specific variable. Such subdivision was allowed because the variables were quantitative types and sorted by normal distribution. Furthermore, sorting out variables, the information within them was unaffected.

We analyzed the variable with the greater value from the previous analysis, as a component that defined a risk, with the risk as the combined result of three factors, hazard, exposure, and vulnerability. We illustrate how to assign a label to each cluster for each variable considered, among the most relevant ones.

We first considered the variable $a_{g,max}$, i.e., the peak ground acceleration for the site, with a return period of 475 years. The first step was the extrapolation of observables in the initial dataset. Subsequently, we associated each observation with the respective cluster indexes and the respective values of $a_{g,max}$. Then, we rearranged the observables in ascending order of $a_{g,max}$, and defined the quartile as the extreme point of the interval. The cluster composition in terms of $a_{g,max}$ is reported in Table 2, together with the resulting assigned labels.

Table 2. Quartile distribution of the $a_{g,max}$ variable in the four clusters.

	%Q1	%Q2	%Q3	%Q4	Label
CL1	74	20	6	0	Low
CL2	0	25	25	50	Medium-to-high
CL3	3	18	68	11	Medium-to-low
CL4	7	16	13	64	High

The labels were assigned based on the percentage prevalence of the cluster for each quartile. A prevalence allocated in the fourth quartile for one of the clusters indicated that the selected cluster gathered the most dangerous municipalities in terms of $a_{g,max}$. On the other hand, a prevalence in the first quartile indicated that the cluster gathered the less dangerous municipalities in terms of seismic hazard.

The same operation was carried out for the hydraulic risk component IDR_POPP2, the prevailing seismic vulnerability variable, i.e., the percentage of buildings under poor maintenance conditions E_30, and the main exposure variable, i.e., density population DENS_POP (see Tables 3–5).

Table 3. Quartile distribution of the IDR_POPP2 variable in the four clusters.

Table

	%Q1	%Q2	%Q3	%Q4	Label
CL1	17	20	54	9	Medium-to-low
CL2	46	41	12	1	Low
CL3	3	5	18	74	Medium-to-high
CL4	4	5	9	82	High

Quartile distribution of the E_30 variable in the four clusters.

	%Q1	%Q2	%Q3	%Q4	Label
CL1	41	27	22	9	Low
CL2	25	30	29	15	Medium-to-low
CL3	18	29	37	16	Medium-to-high
CL4	0	4	11	86	High

Table 5. Quartile distribution of the $a_{g,max}$ variable in the four clusters.

	%Q1	%Q2	%Q3	%Q4	Label
CL1	16	29	40	14	Medium-to-low
CL2	46	28	19	7	Low
CL3	0	0	3	97	High
CL4	5	25	27	43	Medium-to-high

3.2. Overall Risk Definition

Once the variables were rearranged, the incidence of clusters for each variable were calculated and a label for each variable and cluster was assigned (based on the distribution of the cluster indexes within the variable); each cluster was assigned an overall risk label based on their score for each rearranged variable (Table 6).

Table 6. Overall risk quantification for each cluster of municipalities.

	Hydraulic Risk	Seismic Exposition	Seismic Vulnerability	Seismic Hazard	Label
CL1	Medium-to-low	Low	Medium-to-low	Low	Low
CL2	Low	Medium-to-low	Low	Medium-to-high	Low-to-medium
CL3	Medium-to-high	Medium-to-high	High	Medium-to-low	Medium-to-high
CL4	High	High	Medium-to high	High	High

The significance of the assigned risk labels was strictly dependent on the starting population, i.e., from the region under study and do not have absolute value.

This means that the obtained labels cannot be extrapolated to a larger scale without losing their significance. As shown in Figure 11, it is also possible to represent the population of each risk cluster by the main administrative province in the Emilia Romagna region. Obviously, frequency values for each province depend on the number of municipalities, which constitute each province.

Therefore, this plot allows analyzing risk clusters from the same province, but comparing clusters from different provinces may be inappropriate. It is worth noting that the proposed methodology has recognized Piacenza as the province with most low-risk municipalities, while the main cluster featuring Parma, Modena, Bologna, Forlì-Cesena, and Rimini is the low-to-medium risk cluster. Most municipalities of the Reggio-Emilia province are associated with low and low-to-medium clusters. Finally, each of the provinces of Ferrara and Ravenna result being equally split in two main clusters, namely the low and the high-risk clusters in the former case, and the low-to-medium and high-risk clusters in the latter case.

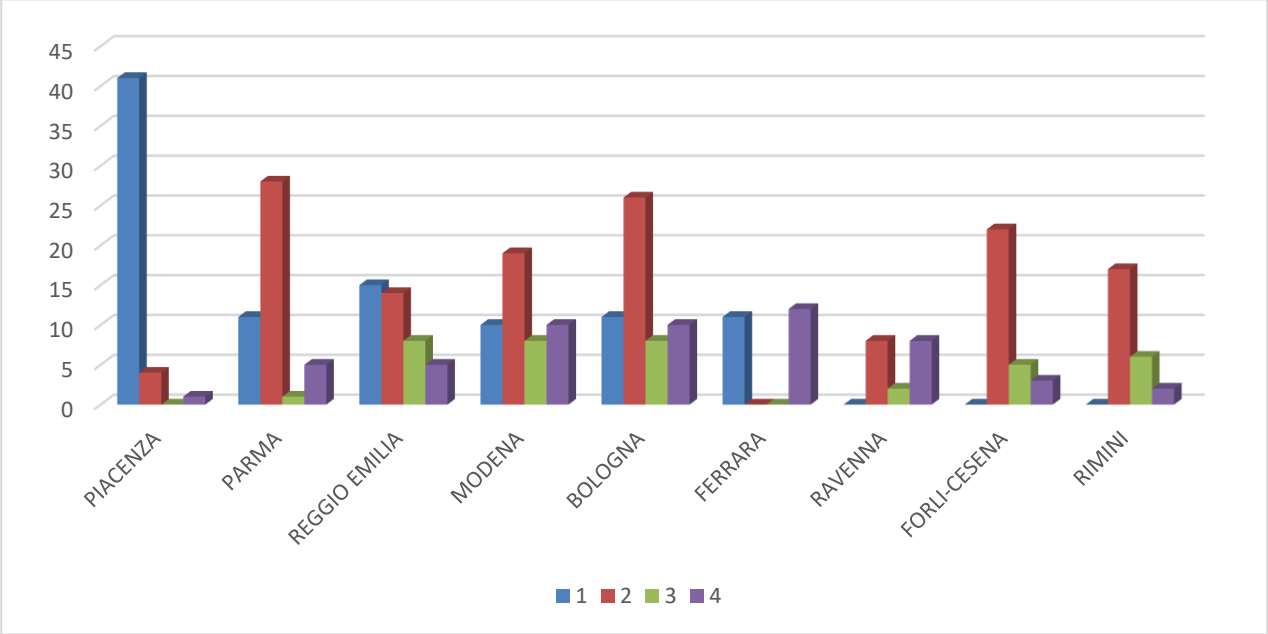

Figure 11. Population of each risk cluster by province in the Emilia Romagna region. In the y-axis, the number of municipalities has been reported.

A.4. Discussion

Ensuring ethical, inclusive, and unbiased machine learning tools is one of the new epistemic frontiers in the application of artificial intelligence technologies to disaster risk management. We recall that this paper discusses an individual application of machine learning tools to a multi-risk assessment of a Northern Italy case study. For this purpose, we had at our disposal a massive amount of data from the ISTAT database containing indicators and data on seismic, hydrogeological, and volcanic risk as well as demographic, housing, territorial and geographical information, obtained through the integration of various institutional sources such as Istat, INGV, ISPRA, Italian Ministry for Cultural Heritage. Like all big data technologies, the adopted machine learning model proved effective in reducing CPU time and model-development costs, owing to its ability to process quantities and sources of data that could not have been otherwise simply elaborated [24,25]. We expect that the model can be used to devise mitigation measures, prepare emergency response, and plan flood recovery measures. The proposed tool has, indeed, the potential for being an operational instrument for land use managers and planners. However, misuse should be avoided, and, for this purpose, crucial issues such as applicability, bias, and ethics should be carefully considered [24–26]. The ethical issues pertaining to a possible misuse of Artificial Intelligence technologies are several [25], including the loss of human decision making, the potential for criminal and malicious use, the emergence of problems of control and use of data and systems, the dependence of the outcomes on users' bias, and the possible prioritization of the "wrong" problems with respect to stakeholder expectations.

Prioritization in disaster multi-risk management, additionally, is markedly affected by needs and expectations of private users, public agencies, and final stakeholders. For instance, a water level management company will be expectedly more inclined to consider flood risk as the most important risk to cope with, while any public agency that is called to reduce the seismic vulnerability of a certain region will tend to consider seismic risk as a priority. Thus, the labeling of the clusterization will be intrinsically permeated with the end-user's intentions. A further aspect is that one should understand that publicizing the results of a multi-risk algorithm might inadvertently touch sensitive aspects from a privacy point of view [27].

In many cases, criticalities rely upon an inherent disconnect between the algorithm's designers and the communities where the research is conducted [26], while users may complain about a lack of transparency and accountability. Furthermore, immature machine learning tools might be used in safety-critical situations for which they are not yet ready. As suggested by Gevaert et al. [26], disaster-risk-management specialists constantly seek expertise on how to clearly communicate the results and uncertainties of machine learning algorithms to reduce inflated expectations. Furthermore, sensitive groups should be identified and audited for overcoming bias. Therefore, we suggest that, before being systematically applied, the present machine learning methodology is validated against established computational modeling tools. We also believe that

the obtained results are very promising, but further efforts are necessary to assess the proneness of the proposed machine learning tool to the aforementioned ethical and bias issues.

A.5. Conclusions

The purpose of this work is to illustrate a sound methodology for the qualitative multi-risk analysis at the regional scale by means of machine learning techniques that allow dealing with large and heterogeneous amounts of data. The initial dataset, made of variables carrying information about hazard, exposure, and vulnerability for both seismic and hydraulic risk for each municipality of the Emilia Romagna region, has been suitably normalized and reduced through the PCA, whereas observations have been clustered through a machine-learning algorithm.

Then, risk labels were individually assigned to clusters for each variable. Finally, based on the score of each variable an overall risk label was assigned to each cluster. Results confirmed previous risk classifications for the case study analyzed. Both provinces with a moderate risk level and high-risk level have been correctly detected by the proposed approach. The reliability of the obtained results is dependent on the existence of valid quantitative initial data for the region under study. In fact, the proposed methodology does not allow qualitative data, whether they are fundamental or not.

In conclusion, the proposed analysis delivers useful information: municipalities with major priority of intervention are identified so that stakeholders can take advantage of this tool to prioritize any preventive measures. Moreover, the procedure also allows identifying the most important variables to consider in a combined seismic and hydraulic multi-risk analysis. In other words, this tool allows evaluating the variables most suited to categorize the observations in terms of combined risk. Indeed, from the analysis, variables have emerged relative to different types of risks, which better communicate with each other and carry most information. By contrast, the methodology also allows identifying variables, which do not collaborate with variables of different nature and, therefore, cannot be usefully employed.

A. Appendix

We provide hereafter a table with the acronyms of the variables used for Figures 5–7:

Table A1. Description of the variables used in Figures 5-7.

DENSPOP	Population Density
AGMAX_50	Maximum ground acceleration (50th percentile) calculated on a grid with a 0.02° step, maximum (MAX) and minimum (MIN) of the values of the grid points falling within the municipal area.
IDR_POPP3	Resident population at risk in areas with high hydraulic hazard-P3

IDR_POPP2	Resident population at risk in areas with medium hydraulic hazard-P2
IDR_POPP	Resident population at risk in areas with low hydraulic hazard-P1
IDR_AREAP1	Areas with low hydraulic hazard P1 (low probability of floods or extreme event scenarios))–D.Lgs. 49/2010 (km^2)
IDR_AREAP2	Areas with average hydraulic hazard P2 (return time between 100 and 200 years)–D.Lgs. 49/2010 (km^2)
IDR_AREAP3	Areas with high hydraulic hazard P3 (return time between 20 and 50 years)-D.Lgs. 49/2010 (km^2)
E5	Residential buildings in load-bearing masonry
E6	Residential buildings in load-bearing reinforced concrete
E7	Residential buildings in other load-bearing materials (steel, wood, ...)
E8	Residential buildings made before 1919
E9	Residential buildings made between 1919 and 1945
E10	Residential buildings made between 1946 and 1960
E11	Residential buildings made between 1961 and 1970
‘E19	Residential buildings with three floors
E20	Residential buildings with more than three floors
E30	Residential buildings with a poor state of conservation
‘E31	Residential buildings with a very poor state of conservation

A.References

1. Fuchs, S.; Keiler, M.; Zischg, A. A spatiotemporal multi-hazard exposure assessment based on property data. *Nat. Hazards Earth Syst. Sci.* 2015, *15*, 2127–2142.
2. Kron, W. Reasons for the increase in natural catastrophes: The development of exposed areas. In *Topics 2000: Natural Catastrophes, the Current Position*; Munich Reinsurance Company: Munich, Germany, 1999; pp. 82–94.
3. Zschau, J. Where are we with multihazards, multirisks assessment capacities? In *Science for Disaster Risk Management: Knowing Better and Losing Less*; Poljansek, K., Marin Ferrer, M., De Groeve, T., Clark, I., Eds.; European Union: Luxembourg, 2017; pp. 98–115.

4. Barthel, F.; Neumayer, E. A trend analysis of normalized insured damage from natural disasters. *Clim. Chang.* 2012, *113*, 215–237.
5. Munich, R.E.; Kron, W.; Schuck, A. Analyses, assessments, positions. In *Topics Geo: Natural Catastrophes*; Münchener Rückversicherungs-Gesellschaft: Munich, Germany, 2014.
6. Peduzzi, P.; Dao, H.; Herold, C.; Mouton, F. Assessing global exposure and vulnerability towards natural hazards: The Disaster Risk Index. *Nat. Hazards Earth Syst. Sci*. 2009, *9*, 1149–1159.
7. Bell, R.; Glade, T. Multi-hazard analysis in natural risk assessments. *WIT Trans. Ecol. Environ*. 2004, *77*, 1–10.
8. Barredo, J.I. Major flood disasters in Europe: 1950–2005. *Nat. Hazards* 2007, *42*, 125–148.
9. Kanamori, H.; Hauksson, E.; Heaton, T. Real-time seismology and earthquake hazard mitigation. *Nature* 1997, *390*, 461–464.
10. Kappes, M.S.; Keiler, M.; von Elverfeldt, K.; Glade, T. Challenges of analyzing multi-hazard risk: A review. *Nat. Hazards* 2012, *64*, 1925–1958.
11. Schmidt, J.; Matcham, I.; Reese, S.; King, A.; Bell, R.; Henderson, R.; Smart, G.; Cousins, J.; Smith, W.; Heron, D. Quantitative multi-risk analysis for natural hazards: A framework for multi-risk modelling. *Nat. Hazards* 2011, *58*, 1169–1192.
12. Gruber, F.E.; Mergili, M. Regional-scale analysis of high-mountain multi-hazard and risk indicators in the Pamir (Tajikistan) with GRASS GIS. *Nat. Hazards Earth Syst. Sci.* 2013, *13*, 2779–2796.
13. Tyagunov, S.; Vorogushyn, S.; Jimenez, C.M.; Parolai, S.; Fleming, K. Multi-hazard fragility analysis for fluvial dikes in earthquake- and flood-prone areas. *Nat. Hazard. Earth Syst. Sci.* 2018, *18*, 2345–2354.
14. Yousefi, S.; Pourghasemi, H.R.; Emami, S.N.; Pouyan, S.; Eskandari, S.; Tiefenbacher, J.P. A machine learning framework for multi-hazards modeling and mapping in a mountainous area. *Sci. Rep.* 2020, *10*, 12144.
15. Boniolo, F.; Dorigatti, E.; Ohnmacht, A.J.; Saur, D.; Schubert, B.; Menden, M.P. Artificial intelligence in early drug discovery enabling precision medicine. *Expert Opin. Drug Discov.* 2021 *16*, 991–1007.
16. Pouyan, S.; Pourghasemi, H.R.; Bordbar, M.; Rahmanian, S.; Clague, J.J. A multi-hazard map-based flooding, gully erosion, forest fires, and earthquakes in Iran. *Sci. Rep.* 2021, *11*, 14889.
17. Pearson, K. On Lines and Planes of Closest Fit to Systems of Points in Space. *Phil. Mag*. 1901, *2*, 559–572.
18. Hotelling, H. Analysis of a complex of statistical variables into principal components. *J. Edu. Psychol*. 1933, *24*, 417–441.
19. Jolliffe, I.T. *Principal Component Analysis*; Springer: New York, NY, USA, 2002.

20. MacQueen, J.B. Some methods for classification and analysis of multivariate observations. In Proceedings of the 5th Berkeley Symposium on Mathematical Statistics and Probability, Berkeley, CA, USA, 1967; University of California Press: Berkeley, CA, USA, pp. 281–297.

21. Ding, C.; Xieofeng, H. K-means clustering via principal components analysis. In Proceedings of the 21st International Conference on Machine Learning, Banff, AB, Canada, 4–8 July 2004; ACM Press: New York, NY, USA, 2004.

22. Trigila, A.; Iadanza, C.; Bussettini, M.; Lastoria, B. *Dissesto Idrogeologico in Italia: Pericolosità e Indicatori di Rischio—Edizione 2018*; Rapporti 287/2018; ISPRA: 2018.

23. Mantovan, L.; Gilli, A. Supplementary Material, Open Access. Available online: https://github.com/alessandrogilli/analisi-multirischio, accessed 15/10/2021.

24. Wagenaar, D.; Curran, A.; Balbi, M.; Bhardwaj, A.; Soden, R.; Hartato, E.; Sarica, G.M.; Ruangpan, L.; Molinario, G.; Lallemant, D. Invited perspectives: How machine learning will change flood risk and impact assessment. *Nat. Hazards Earth Syst. Sci.* 2020, *20*, 1149–1161.

25. Stahl, B.C. Ethical Issues of AI. Artificial Intelligence for a Better Future: An Ecosystem Perspective on the Ethics of AI and Emerging Digital Technologies. In *SpringerBriefs in Research and Innovation Governance*; Springer: Berlin/Heidelberg, Germany, 2021; pp. 35–53.

26. Gevaert, C.M.; Carman, M.; Rosman, B.; Georgiadou, Y.; Soden, R. Fairness and accountability of AI in disaster risk management: Opportunities and challenges. *Patterns* 2021, *2*, 100363.

27. GFDRR. *Machine Learning for Disaster Risk Management*; GFDRR: Washington, WA, USA, 2018.

PART B: PROMETHEE analysis

Social vulnerability is deeply affected by the increase in hazardous events such as earthquakes and floods. Such hazards have the potential to greatly affect communities, including in developed countries. Governments and stakeholders must adopt suitable risk reduction strategies. This study is aimed at proposing a qualitative multi-hazard risk analysis methodology in the case of combined seismic and flood risk using PROMETHEE, a Multiple-Criteria Decision Analysis technique. The present case study is a multi-hazard risk assessment of the Ferrara province (Italy). The proposed approach is an original and flexible methodology to qualitatively prioritize urban centers affected by multi-hazard risks at the regional scale. It delivers a useful tool to stakeholders involved in the processes of hazard management and disaster mitigation.

B.1. Premise on the use of PROMETHEE

Many areas in Europe and worldwide are increasingly subjected to catastrophic events. These events intensify the exposure of these territories to multi-risk events and make societies more vulnerable to entangled risks [1–7]. Globalization and climate changes are the main culprits of these multi-risk dynamics. Globalization, indeed, makes countries closely linked and interdependent, so communities are not only vulnerable to local extreme events but also to those occurring outside their national territories. Climate change increases, among others, the frequency and intensity of extreme meteorological phenomena, hydrological and flood risk, as well as the risk of fires. The awareness of this worrying trend has determined the need for adequate tools to address and mitigate these risks, as well as information campaigns to foster resilience and coping capacity of communities [5–7].

Understanding risks involving vast inhabited areas is therefore paramount, particularly when assessing potential losses produced by a combination of multiple hazards. Hereafter, a hazard refers to the probability of occurrence in a specified period of a potentially damaging event of a given magnitude in a given area [8]. Total risk is a measure of the expected human (casualties, injuries) and economic (damage to property, activity disruption) losses due to adverse natural phenomena. Such a measure is assumed to be the product of hazard, vulnerability, and exposure instances [9]. Many areas on Earth are subjected to the effects of coexisting multiple hazards, among which floods [3,8] and earthquakes are some of the most widespread [5–7]. Though inhabited environments are affected by multiple hazardous processes, most studies focus on a single hazard [8].

The choice to adopt a multi-risk analysis approach has the potential to play a fundamental role in increasing urban resilience, an essential factor for sustainable development, enabling cities to prepare, respond, and recover when hit by catastrophic events, and therefore prevent or contain economic, environmental, and social losses [1]. However, performing a multi-risk analysis with the tools and methodologies available today raises numerous challenges and difficulties [10–20]. For instance, an updated analysis of multi-hazard aggregated risk for infrastructures considering multiple potential threats has recently been proposed in reference [5].

Risk assessment is indeed carried out through independent procedures that adopt different estimation metrics. This makes comparisons difficult and precludes considering correlations or cascading effects [11]. On the contrary, the Multiple-Criteria Decision Analysis (MCDA) technique is a promising approach in multiple-hazard risk analysis, even if this route has been scarcely explored to date [21–24].

To pave the way for sustainable land-use plans and risk-mitigation strategies, we must analyze, quantify, and, especially, compare all concurrent risks [25]. To date, single-risk assessment is generally performed by means of independent procedures, whose results cannot be compared. The purpose of this paper is to devise an approach for the qualitative assessment of combined risks at the regional scale. In particular, the objective is to jointly analyze the flood and seismic risk for the Ferrara province area. The proposed approach is based on the suitable use of the Preference Ranking Organization Method for Enrichment Evaluations (PROMETHEE), a Multiple-Criteria Decision Analysis technique [26–29]. The province of Ferrara is in a flatland area in the northern part of Italy. Historically, it has been mainly hit by floods and seismic events. Though floods are exogeneous processes, whereas earthquakes are exogenic, we assume flood and seismic hazards to be the two relevant hazards for determining a priority list. This priority list is meant to be useful to stakeholders and public agencies called to rapidly implement investment plans aimed to prevent economic and life losses and foster the coping capacity of communities to manage the adverse conditions induced by natural disasters. Particularly, the present objective is to prioritize this among the different municipalities. Therefore, the adopted level of observation is at the scale of the area included within each municipality.

Assuming the municipalities of the province of Ferrara as the alternatives of the multiple-criteria analysis, the proposed approach defines a priority ranking among all the alternatives. The outcome is represented by qualitative risk maps. These maps are useful tools for stakeholders involved in community management and risk prevention.

Among the Multi-Risk Methodologies applied in Italian territories, we recall here the works by Gallina et al. [23,24] for the assessment of the impact of sea-level rise, coastal erosion, and storm surge induced by climate changes in coastal zones in North Italy. Flood and seismic risks have been multi-assessed through a Machine Learning framework recently devised by the authors for the Emilia Romagna region [30]. Up to now, the present contribution is the very first to use an MCDA approach for multi-risk analysis of combined flood and earthquake risks, while no other relevant contributions exist dealing with multi-hazard analyses of the Province of Ferrara.

B.2. Materials and Methods

B2.1. Geographical Context and Single Risk Description

To introduce the concept of multi-risk assessment, it is first necessary to discuss the concept of single risk. Risk is basically defined as the product of three parameters: Hazard, vulnerability, and exposure [9]. A hazard represents the probability that an adverse event will occur in a specific area and in a specific time interval. Vulnerability, on the other hand, is an intrinsic characteristic of a system; it represents its propensity to suffer a certain level of damage following the occurrence of a hazard event. Finally, exposure indicates the presence of people, critical infrastructures, natural and cultural heritage, and much more still in hazard zones that are thereby subject to potential losses [4].

The concept of multi-risk follows as the overall risk from a multi-hazard and multi-vulnerability perspective. The term multi-hazard indicates several hazards affecting the same exposed elements (with or without space–time coincidence) or the occurrence of a hazard event that triggers another one giving rise to a domino or cascade effect. Furthermore, the term multi-vulnerability indicates those circumstances where several elements are sensitive to different possible vulnerabilities towards the various hazards affecting them or vulnerabilities that vary over time [10,11].

The territory of the province of Ferrara is located at the north-eastern extremity of the Padana Plain, a flat land area in the north part of Italy crossed by the Po River and bathed by the Adriatic Sea on the east side. It is characterized by minimum land slopes and its altimetry is mainly under the mean sea level, as almost half of its area is below the mean sea level, as shown in Figure 1. Moreover, the eastern part of the territory is affected by subsidence phenomena as well. These

ground-level modifications, caused mainly by anthropogenic actions as well as by geological and neotectonic factors [31,32], produced a subsidence rate of up to −2.5 mm/year [31]. The main watercourses that flow through the Ferrara province are the Po River, which marks the northern border of the Reno River, and the Idice and Sillaro streams, which are not tributaries of the Po River, and cross the province in their last stretch. Furthermore, numerous artificial canals flow through the Ferrara Province, including the Cavo Napoleonico, which connects the Po and Reno rivers, and the Idrovia Ferrarese.

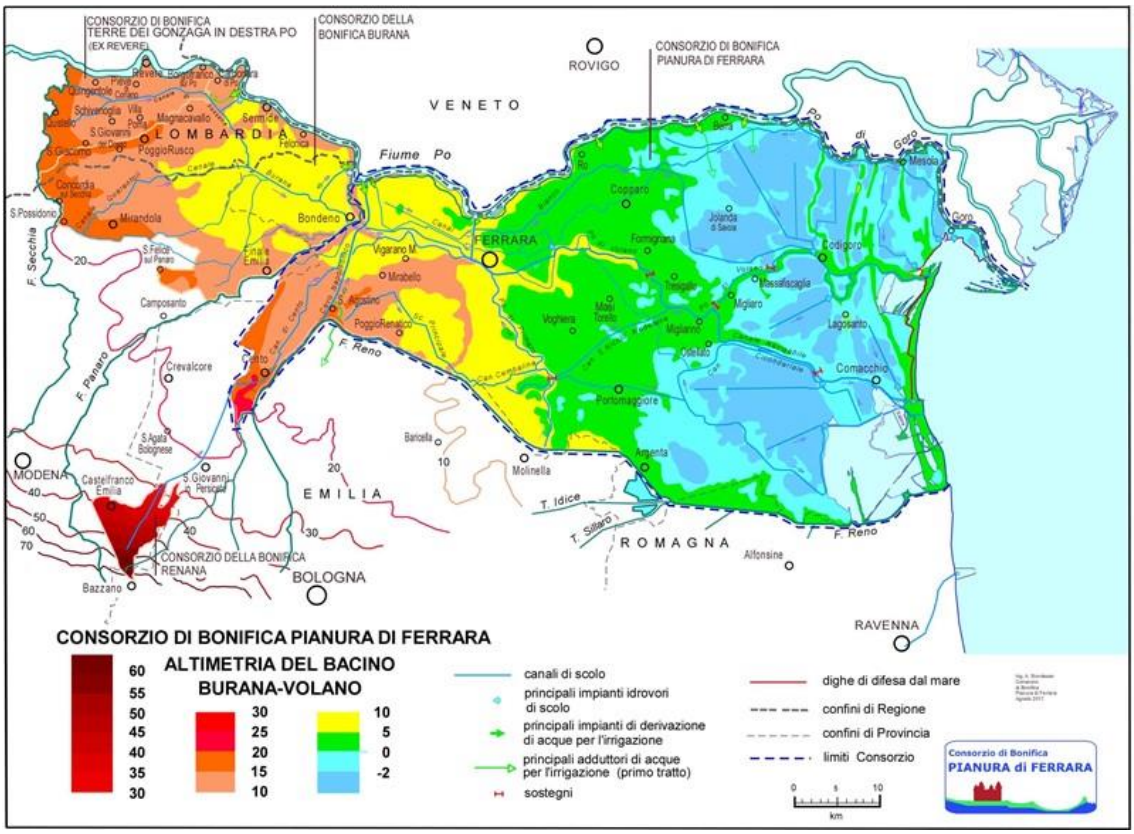

Figure 1. Altimetric map of Ferrara province (free source https://www.bonificaferrara.it/images/Allegati/SITL/4d-3-altimetria(100).pdf, accessed 3 January 2022, made available by Consorzio di Bonifica Pianura di Ferrara). The minimum and maximum extremal values of the ground level over the sea in the legend are −2 m (dark blue) and 60 m (dark red), respectively.

The province of Ferrara includes 23 municipalities. Attention is hereafter restricted to the two main risks of the area under study, namely flood and seismic risks. Site effects associated with

inherent geological morphology and instability issues such as liquefaction were not considered, for simplicity. Desertification is another risk that has been emerging in recent years in the Po delta plain [10]. However, it has not been considered in the present contribution. Hereafter, flood risk refers to the risk that depends on the probability of occurrence of a flood, evaluated concerning the different typologies of watercourses that flow through the territory. The flood risk for the selected region was quantified by the Land Reclamation Authority of the province of Ferrara (Consorzio di Bonifica Pianura di Ferrara), and accounts for flood hazard, exposure, and vulnerability parameters.

Seismic risk depends on the peak ground acceleration (PGA) as well as on the vulnerability of the built environment and the exposure of people and economic activities. We exploited the map of seismic hazard provided by the Italian Institute of Volcanology and Geophysics (INGV), and the seismic classification of municipalities in Emilia (free source https://ambiente.regione.emilia-romagna.it/en/geologia/seismic-risk/seismic-classification, last accessed 28 January 2022), shown in Figure 2a. In Figure 2b, Italy is divided into different areas according to peak ground acceleration values [33] (free source http://zonesismiche.mi.ingv.it/, last accessed on 28 January 2022).

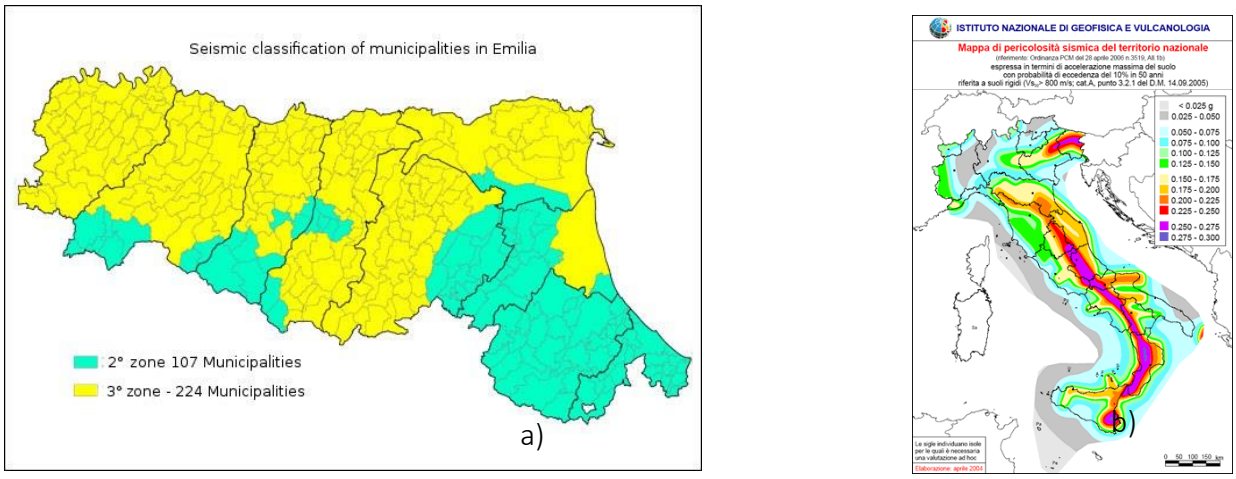

Figure 2. (**a**) Seismic classification of municipalities in Emilia (https://ambiente.regione.emilia-romagna.it/en/geologia/seismic-risk/seismic-classification, accessed 28 January 2022). (**b**) Seismic Hazard Map of Italy (free source from INGV webpage http://zonesismiche.mi.ingv.it/, accessed on 28 January 2022).

Finally, we used the database made available by the Italian National Institute of Statistics (Istat). This database was used in 2018 by the Italian Superior Institute for Environmental Protection and

Research (ISPRA) to produce seismic, hydrogeological, volcanic, and social vulnerability hazard maps for the entire Italian peninsula. The reader is referred to the pertinent report by Trigila et al. [34] to obtain a detailed description of ISPRA's methodology for the processing of the data.

2.2. The PROMETHEE Method

The proposed multi-hazard risk analysis procedure for the region under study is based on PROMETHEE [26–29], a Multiple-Criteria Decision Analysis method. It belongs to the class of aggregation methods based on outranking relationships. It is known for its simplicity and the ability to analyze information from multiple sources. PROMETHEE allows one to jointly compare data originally expressed in different units and scales. A flux diagram explaining the various steps of the PROMETHEE-based analysis can be found in reference [29].

PROMETHEE deals with maximization or minimization problems with k different criteria of the kind

$$\max(or\ \min)\{g_1(a), g_2(a), ..., g_k(a) \mid a \in A\}, \tag{1}$$

where A is a finite set of possible alternatives and function $g_j(a)$ represents the performance of the *j*-th criterion. Let us consider two alternatives, $(a,b) \in A.$ We have the following cases:

$$\begin{cases} \forall j : g_j(a) \geq g_j(b) \\ \exists k : g_k(a) > g_k(b) \end{cases} \Leftrightarrow aPb,$$

$$\forall j : g_j(a) = g_j(b) \Leftrightarrow aIb, \tag{2}$$

$$\begin{cases} \exists s : g_s(a) > g_s(b) \\ \exists r : g_r(a) < g_r(b) \end{cases} \Leftrightarrow aRb,$$

Generalized Criterion	Definition	Parameters to Fix
Type 1: usual criterion	$P(d)=\begin{cases}0 & d\le 0\\ 1 & d>0\end{cases}$	-
Type 2: U-shape criterion	$P(d)=\begin{cases}0 & d\le q\\ 1 & d>q\end{cases}$	q
Type 3: V-shape criterion	$P(d)=\begin{cases}0 & d\le p\\ \frac{d}{p} & 0\le d\le p\\ 1 & d>p\end{cases}$	p
Type 4: Level criterion	$P(d)=\begin{cases}0 & d\le q\\ \frac{1}{2} & q\le d\le p\\ 1 & d>p\end{cases}$	p, q
Type 5: V-shape with indifference criterion	$P(d)=\begin{cases}0 & d\le q\\ \frac{d-q}{p-q} & q\le d\le p\\ 1 & d>p\end{cases}$	p, q
Type 6: Gaussian criterion	$P(d)=\begin{cases}0 & d\le 0\\ 1-e^{-\frac{d^2}{2s^2}} & d>0\end{cases}$	s

where *P*, *I,* and *R* denote preference (*P*), indifference (*I*), or incompatibility relations (*R*) of one alternative over the other, respectively.

Table 1. Types of preference function.

By comparing all the alternatives for each criterion, a hierarchy of alternatives belonging to the starting space A will be obtained. When comparing two actions, $(a,b)\in A.$ the result of this comparison is expressed in terms of the preference function $\wp:A\times A\to(0,1)$ that represents the intensity of the preference of alternative *a* towards alternative *b*. Therefore, $\wp(a,b)=0$ indicates no preference of *a* over *b* (or indifference), $\wp(a,b)\simeq 0$ indicates a weak preference of *a* over *b*, $\wp(a,b)\simeq 1$ indicates a strong preference of *a* over *b,* and $\wp(a,b)=1$ indicates a strict preference

of *a* over *b*. In practice, the preference function will often be a function of the difference between the evaluations of the two alternatives considered:

$$\wp(a,b) = P(g(a) - g(b)) = P(d), \tag{3}$$

where *P* is a non-decreasing function, equal to zero for negative values of *d*. PROMETHEE offers six types of preference functions (see Table 1).

Therefore, a preference index is defined as follows:

$$\begin{cases} \pi(a,b) = \sum_{j=1}^{k} P_j(a,b) w_j \\ \pi(b,a) = \sum_{j=1}^{k} P_j(b,a) w_j \end{cases}, \tag{4}$$

where $\pi(a,b)$ expresses the degree to which *a* is preferred to *b* over all criteria and vice versa, and w_j is the weight of each criterion and expresses a measure of the importance of the relative criterion.

For all the criteria, a classification is available for the various alternatives necessary to define the so-called outranking flows, which are the fundamental units for the PROMETHEE methodology. Each alternative *a* faces $(n-1)$ other alternatives that belong to the generic space A. The two following outranking flows are defined:

$$\begin{cases} \Theta^{+}(a) = \frac{1}{n-1} \sum_{x \in A} \pi(a,x) \\ \Theta^{-}(a) = \frac{1}{n-1} \sum_{x \in A} \pi(x,a) \end{cases}, \tag{5}$$

where *x* represents the deviation of the specific preference function with respect to the same function of preference for the other alternatives. $\Theta^{+}(a)$ expresses how alternative *a* outranks all the others, otherwise $\Theta^{-}(a)$ expresses how alternative *a* is outranked by all the others. The higher $\Theta^{+}(a)$ (lower $\Theta^{-}(a)$) is, the more likely alternative *a* is strongest; otherwise, alternative *a*, compared to the others, is weakest when $\Theta^{+}(a)$ assumes small values. Once these two flows have been defined, it becomes very simple to make comparisons between alternatives and subsequently establish their order.

PROMETHEE offers several ways to view the results; the main ones are illustrated below:

PROMETHEE I Partial Ranking: This is a partial ranking of the alternatives, based on positive and negative flows, and includes preferences, indifference, and incomparability. This scheme allows, therefore, to compare, where possible, the alternatives and establish their partial order of preference through the indices and the related outranking flows.

PROMETHEE II Complete Ranking: This is useful when the decision maker needs a complete hierarchy among the alternatives of the problem. In this case, the alternatives will be compared in relation to their net flow $\Theta(a) = \Theta(a)^{+} - \Theta^{-}(a)$. PROMETHEE II allows a complete classification of the alternatives; however, it is less realistic and poor in information as it eliminates any possible factor of incomparability between the different alternatives.

PROMETHEE Table: This displays the Θ , Θ^{+}, and Θ^{-} scores. The actions are ranked according to the PROMETHEE II complete ranking.

PROMETHEE Rainbow: This is a diagram that allows one to highlight, for each alternative, the criteria that positively or negatively affect the final result.

Profile of alternatives: This is a diagram that shows, for each alternative, the net flow Θ of each criterion.

B.2.3. Data Collection and Processing

Both flood and seismic risks have been included in PROMETHEE as criteria according to their components (hazard, exposure, and vulnerability), while the municipalities, i.e., the object on which to evaluate the criteria, are the alternatives. Risk parameters for each municipality are made available by the National Institute of Vulcanology and Geophysics (INGV), the Italian National Institute of Statistics (Istat), and the Land Reclamation Authorities of the Province of Ferrara. Accordingly, we have drawn from the aforementioned databases a simplified map of the flood risk. In particular, Figure 3 displays the flood hazard for the Province of Ferrara in terms of the probability of floods. In this map, the classification is based on Italian Government Decree n. 49/2010 [35]. Accordingly, frequent floods are defined as those having a high probability of occurrence, with a return period of $20 \leq T \leq 50$ years (P3); infrequent floods have an average probability of occurrence with a return period of $100 \leq T \leq 200$ years (P2); finally, low-probability floods have a return period of $200 < T \leq 500$ years (P1).

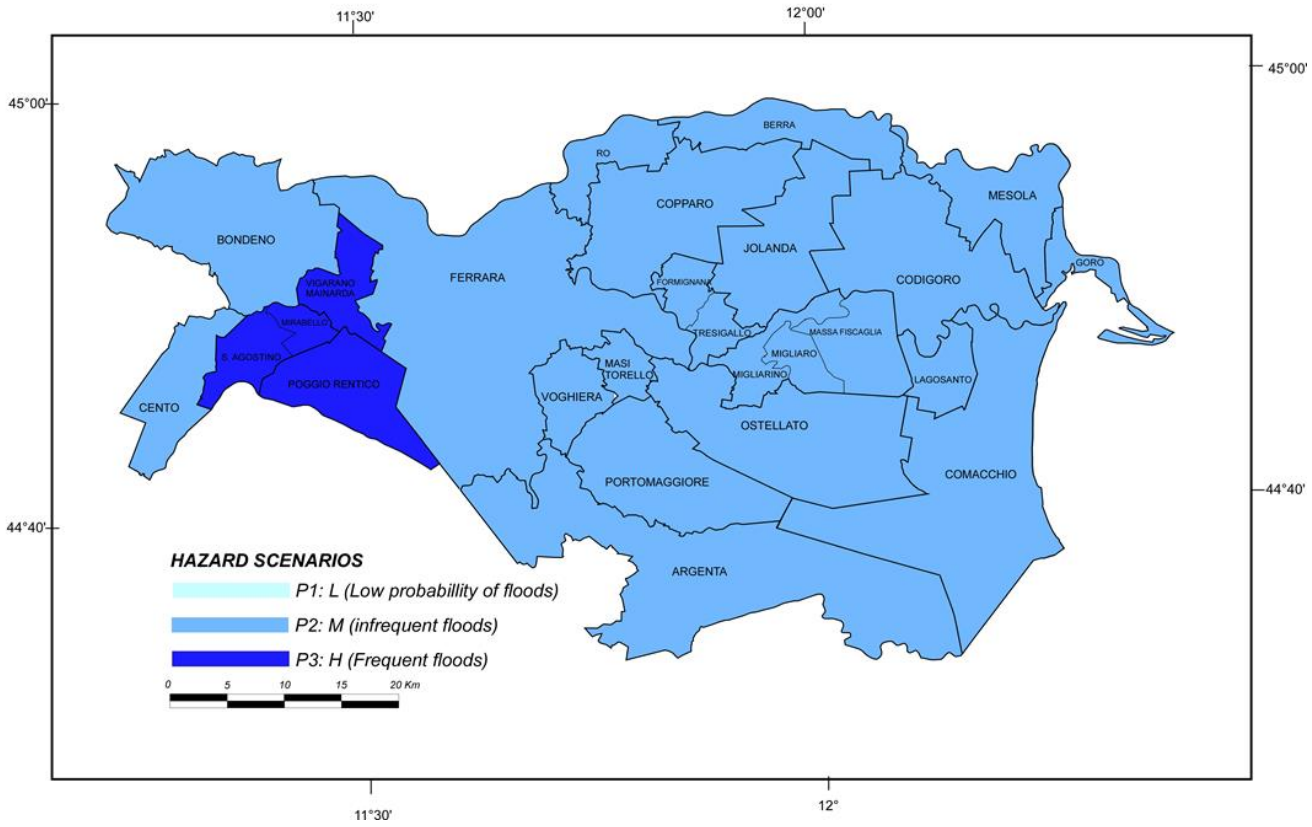

Figure-3. Map of the flood hazard for the province of Ferrara in terms of probability of flood.

Figure 4 provides a map of the seismic hazard for the province of Ferrara in terms of peak ground acceleration (PGA). The PGA-intervals are indicated in the legend.

As for exposure-related criteria, for each municipality, we adopted three parameters: Land use percentage, the number of strategic buildings, and population density. All of them were drawn from the Istat database. The strategic buildings were defined based on the presence and number of halls, police stations, fire brigade buildings, schools, universities, water lifting plants, hospitals, and civil protection centers. This information was obtained from the website of the province of Ferrara (http://www.provincia.fe.it/, 1 October 2021), as per educational and public institutions and centers, and from the website of the Consorzio di Bonifica Pianura di Ferrara as per water lifting plants (https://www.bonificaferrara.it/, 1 October 2021).

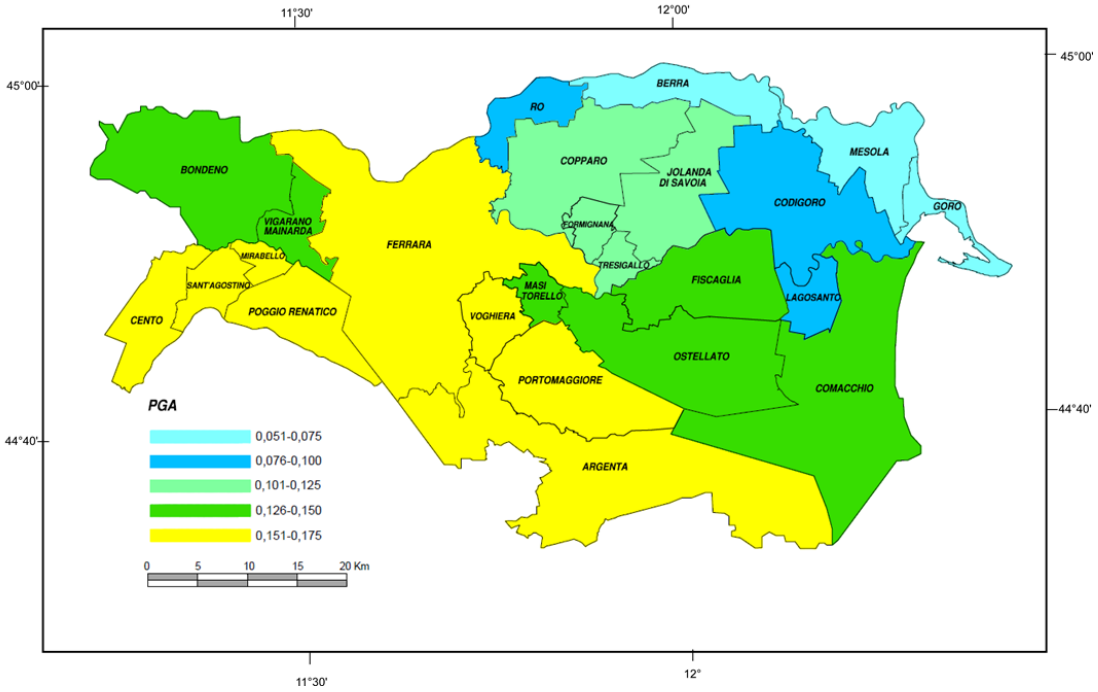

Figure 4. Map of the seismic hazard for the province of Ferrara in terms of peak ground acceleration.

Specifically, four classes of land use percentages were obtained based on the ratio between the urbanized area divided by the total area. In synthesis, we collected the municipalities into four land use classes (Figure 5), four classes in terms of the number of strategic buildings (Figure 6), and four classes of population density (Figure 7).

As for the vulnerability criteria, we adopted a single non-dimensionalized parameter, which accounts for the average age of buildings. Knowing the age of construction and the corresponding number of buildings, we computed the following vulnerability index:

$$I_v = \frac{A\,\alpha_1 + B\,\alpha_2 + C\,\alpha_3 + D\,\alpha_4}{A+B+C+D},$$

where $A, B, C\ e\ D$ represent the number of buildings built between the end of 1800 and 1945; the number of buildings built between 1946 and 1980; the number of buildings built between 1981 and 2000, and finally, the number of buildings built from 2001 up to now. $\alpha_1,\ \alpha_2, \alpha_3\ e\ \alpha_4$ are coefficients equal to 1, 0.75, 0.5, and 0.25, respectively. The vulnerability index I_v results in being mainly related to the age of buildings, and its map is shown in Figure 8.

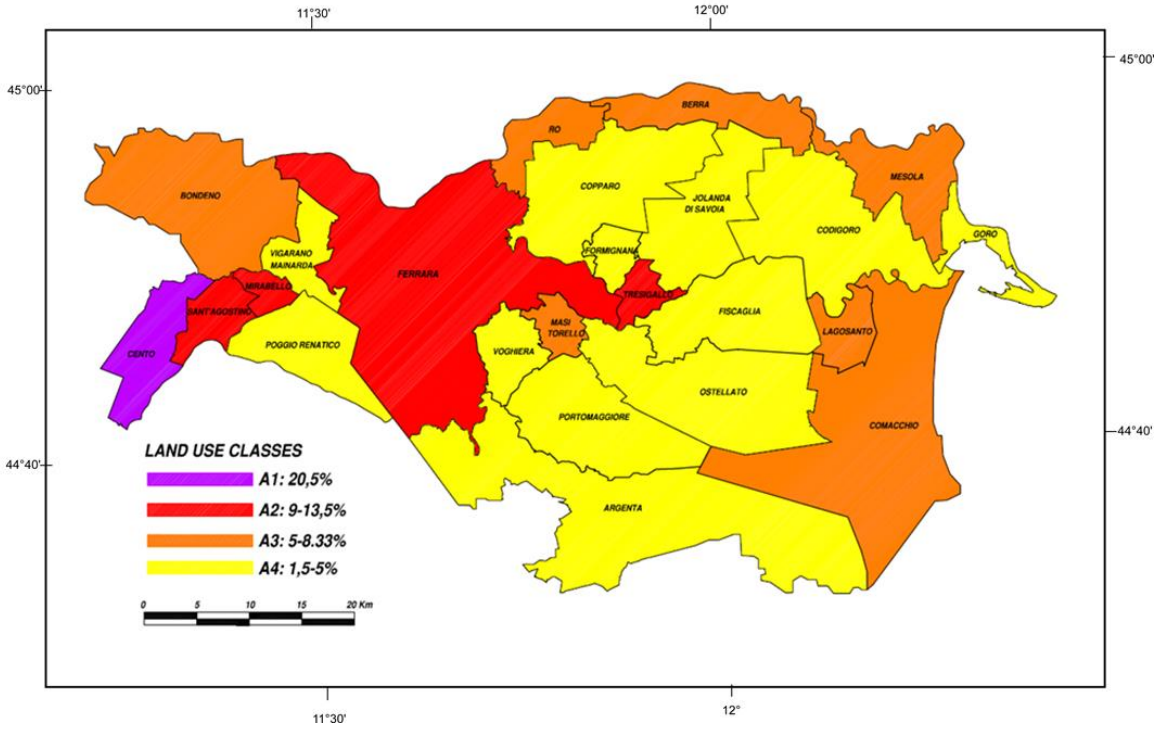

Figure 5. Land use map for the province of Ferrara.

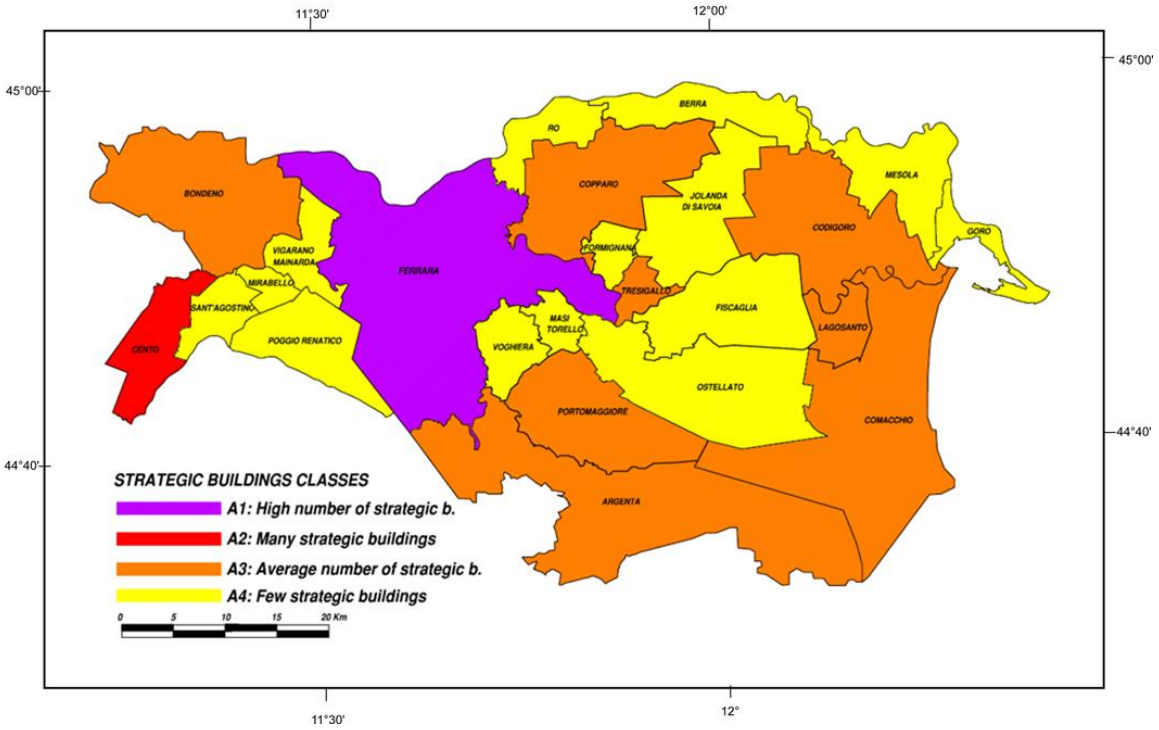

Figure 6. Map of strategic buildings incidence for the province of Ferrara.

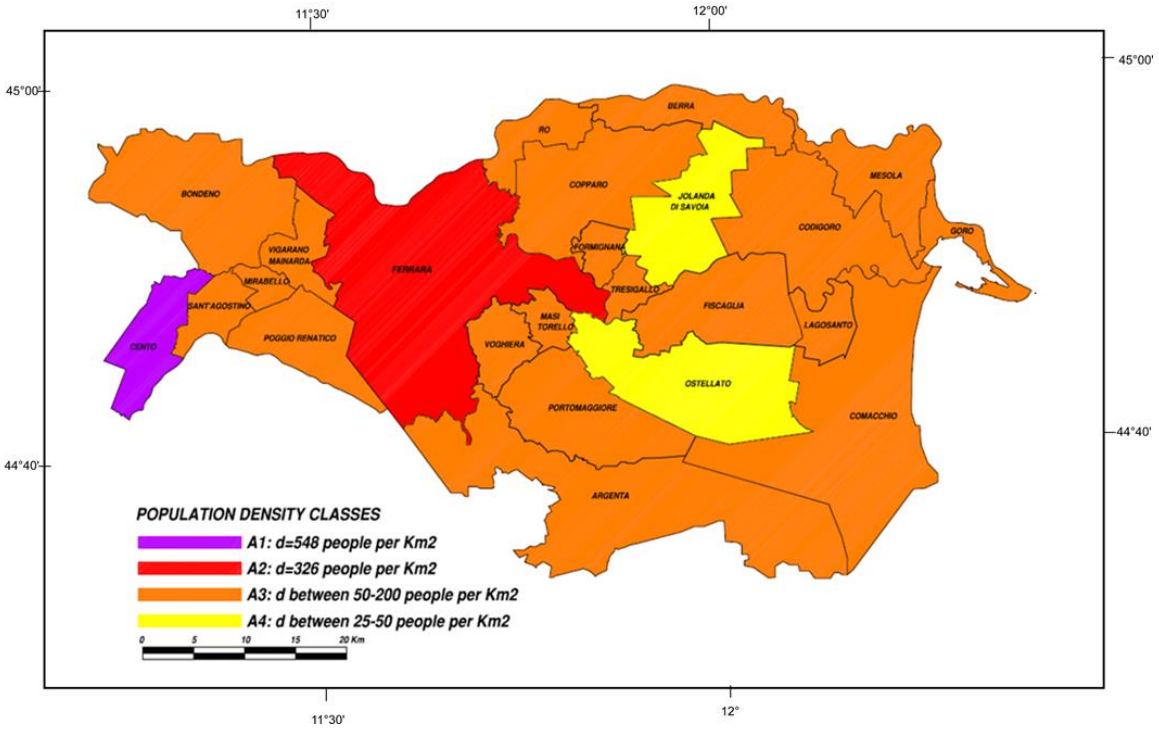

Figure 7. Map of the population density for the province of Ferrara.

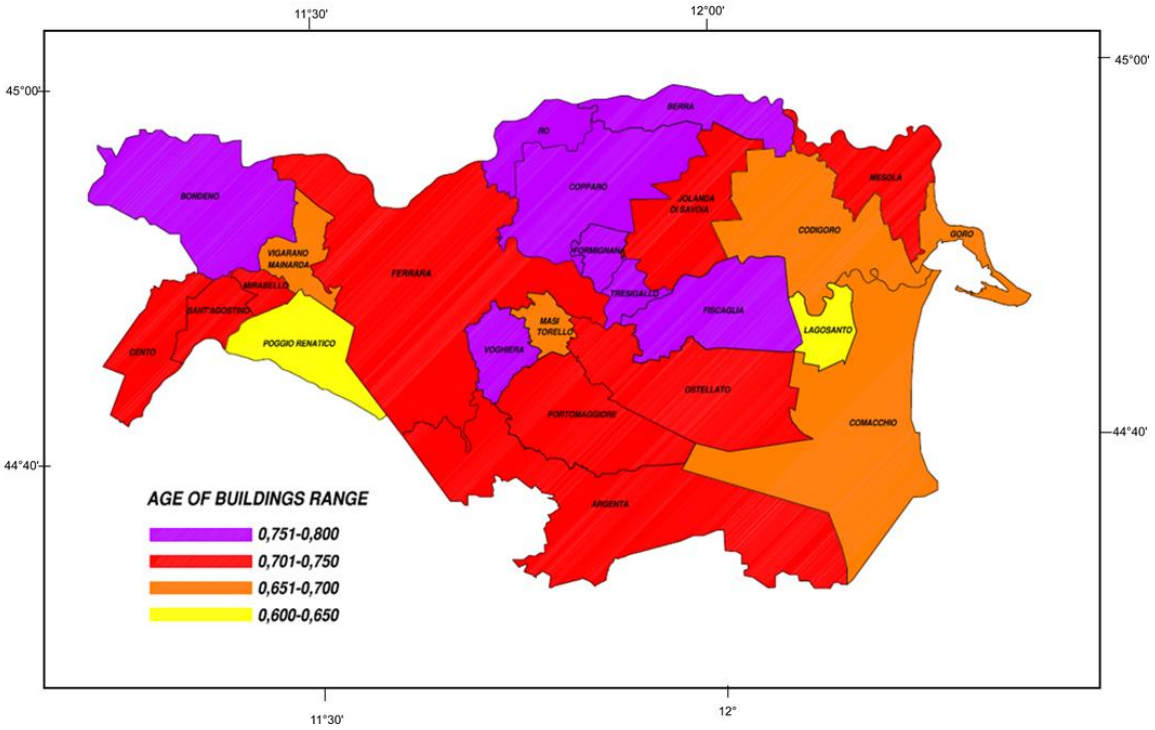

Figure 8 Map of the vulnerability parameter for the province of Ferrara computed as a function of the building age.

B.2.4. Normalization and Weight Assignment

All the data have been collected in an evaluation matrix, whose rows correspond to each alternative (i.e., each municipality), while each column corresponds to each selected criterion. In other words, the *i,j*-th element of the evaluation matrix expresses the value of the *i*-th alternative relating to the attribute of the *j*-th criterion and describes the performance of each alternative regarding each criterion.

It should be noted that criteria are represented through different scales and units. This precludes mutual comparisons. Thus, it is necessary to further homogenize the data contained in the evaluation matrix and proceed with comparisons through normalization. Through the preference function, the performance of the alternatives is transformed into a dimensionless value, ranging from o to 1. As a first attempt, we adopted the Type 1 preference function described in Table 1, which does not require the definition of any threshold. Subsequently, the linear preference function was also used.

Finally, we attributed weights to each criterion. Through this step, decision makers can make their preferences explicit, since it is not ensured that all the criteria take on the same importance. We first decided to attribute the same weight to each criterion. Then, a sensitivity analysis was performed with varying weights.

The risk maps shown in the following sections indicate three classes of risk levels, namely low, medium, high. It is emphasized that this classification must be intended as a pure ranking in terms of the relative urgence of investments. It does not at all intend to indicate the level of safety in absolute terms of the various municipalities. This classification answers the question as to whether the method can provide the priority level associated with a certain municipality and help to decide how to distribute investments over various municipalities.

B.2.5. Sensitivity Analysis

To verify the reliability of the results obtained, a sensitivity analysis was carried out. During this sensitivity analysis, we retraced the procedure by which the results were obtained and identified the steps most affected by uncertainties and subjectivity, considering their influence on the final ranking. Specifically, the choice of the preference function and the choice of weights appeared to be the most subjective. As for the choice of the preference function, a previous study [26] recommends assuming a linear preference function endowed with the definition of *p*, *q* thresholds. Two approaches are adopted for the determination of *p* and *q*: The so-called zero-max method, which imposes that the indifference threshold *q* is assigned the value of zero while the preference threshold *p* is set to be equal to the maximum difference between the evaluations of the criteria.

Table 2. Preference functions and the associated thresholds *p*, *q,* and *s*.

	Criteria					
	Flood Hazard	PGA	Land Use	Strategic Buildings	Age Buildings	ofPopulation Density
Min/Max	max	Max	max	max	max	max
Weight	1	1	1	1	1	1
Preference function	Usual	Linear	Linear	Usual	Linear	Linear

Thresholds	absolute	Absolute	absolute	absolute	absolute	absolute
Sensitivity analysis: increase						
Scenario 0	All p =					
Scenario 1	Inc co $p_i = 25.5\%$ $p_{\text{other criteria}} = 14.9\%$					
	n/a	0.000	0.0000	n/a	0.000	0.000
Scenario 2	Inc co $p_i = 38.2\%$ $p_{\text{other criteria}} = 12.3\%$					
Scenario 3	Inc co $p_i = 57.4\%$ $p_{\text{other criteria}} = 8.5\%$					
q: Indifference, zero-max						
p: Preference (zero-max)	n/a	0.098	0.1896	n/a	0.158	523.00
s: Gaussian (zero-max)	n/a	n/a	n/a	n/a	n/a	n/a
q: Indifference (mean-std)	n/a	0.093	0.0261	n/a	0.0676	16.10
p: Preference (mean-std)	n/a	0.155	0.1081	n/a	0.766	238.60
s: Gaussian (mean-std)	n/a	n/a	n/a	n/a	n/a	n/a

The mean-std method requires the calculation of the average value and the standard deviation of a set of differences between the evaluations of the criteria. In the mean-std method, the

indifference threshold is assigned the value of the difference between the average value and standard deviation, while the sum between the average value and standard deviation is assigned to the preference threshold. Following [26–28], we adopted the preference function of the linear type for the quantitative criteria, that is flood hazard, land use, the age of buildings, and population density. However, the algorithm was also run by choosing the usual preference function, which is the simplest possible one. The thresholds were computed as shown in Table 2. As for the sensitivity on the weights, the four scenarios described in Table 3 have been considered.

B.3. Results

In the following Section, we describe the outcomes of the multiple-criteria analysis for the usual and linear preference function as well as the results of the sensitivity analysis performed for varying weight changes.

B.3.1. Usual Preference Function

When the usual preference function is used, the algorithm assumes equal weights. We recall that, here, thresholds *p* and *q* are not required. Basically, what is provided to the analyst is an order of priority where the municipalities in the province of Ferrara are ordered from the most sensitive to combined flood and seismic risk to the one that is least affected. Table 4 shows the final ranking of the alternatives.

This is not the only way to visualize the results: The PROMETHEE rainbow plot, shown in Figure 9, allows one to highlight, for each alternative, the criteria that positively or negatively affect the results. In Figure 9, the colors are representative of the criterion: Yellow indicates the criteria relating to exposure, red is used for seismic hazard, green for vulnerability, and blue for flood hazard. For example, for the municipality of Ferrara (first in the ranking), it can be observed that the criterion that has a negative effect is the one relating to the flood hazard, whereas the other criteria have a positive effect on the Ferrara municipality. On the contrary, in the municipality of Jolanda di Savoia (last in the ranking), the only criterion that has a positive influence is the one relating to vulnerability, while all the others have a negative influence.

Table 3. Sensitivity analysis on the weights of the criteria.

Rank	Alternatives	Θ	Θ^+	Θ^-

1	Ferrara	0.6111	0.7302	0.119
2	Cento	0.5873	0.7222	0.1349
3	Tresigallo	0.4127	0.6111	0.1984
4	Vigarano Mainarda	0.2857	0.5873	0.3016
5	Mirabello + Sant'Agostino	0.2698	0.5794	0.3095
6	Argenta + Portomaggiore	0.2381	0.5238	0.2857
7	Bondeno	0.1825	0.4921	0.3095
8	Copparo	0.0238	0.4127	0.3889
9	Poggio Renatico	0.0238	0.4524	0.4286
10	Comacchio	0.0000	0.4048	0.4048
10	Formignana	0.0000	0.381	0.381
12	Voghiera	−0.0238	0.3651	0.3889
13	Lagosanto	−0.0317	0.3889	0.4206
14	Berra	−0.1587	0.3016	0.4603
15	Masi Torello	−0.1746	0.2937	0.4683
16	Ro	−0.1905	0.2857	0.4762
17	Fiscaglia	−0.2063	0.2778	0.4841
18	Mesola	−0.2857	0.2381	0.5238
19	Ostellato	−0.3571	0.1984	0.5556
20	Goro	−0.3651	0.1984	0.5635
21	Codigoro	−0.3651	0.2222	0.5873

22	Jolanda di Savoia	−0.4762	0.1429	0.619

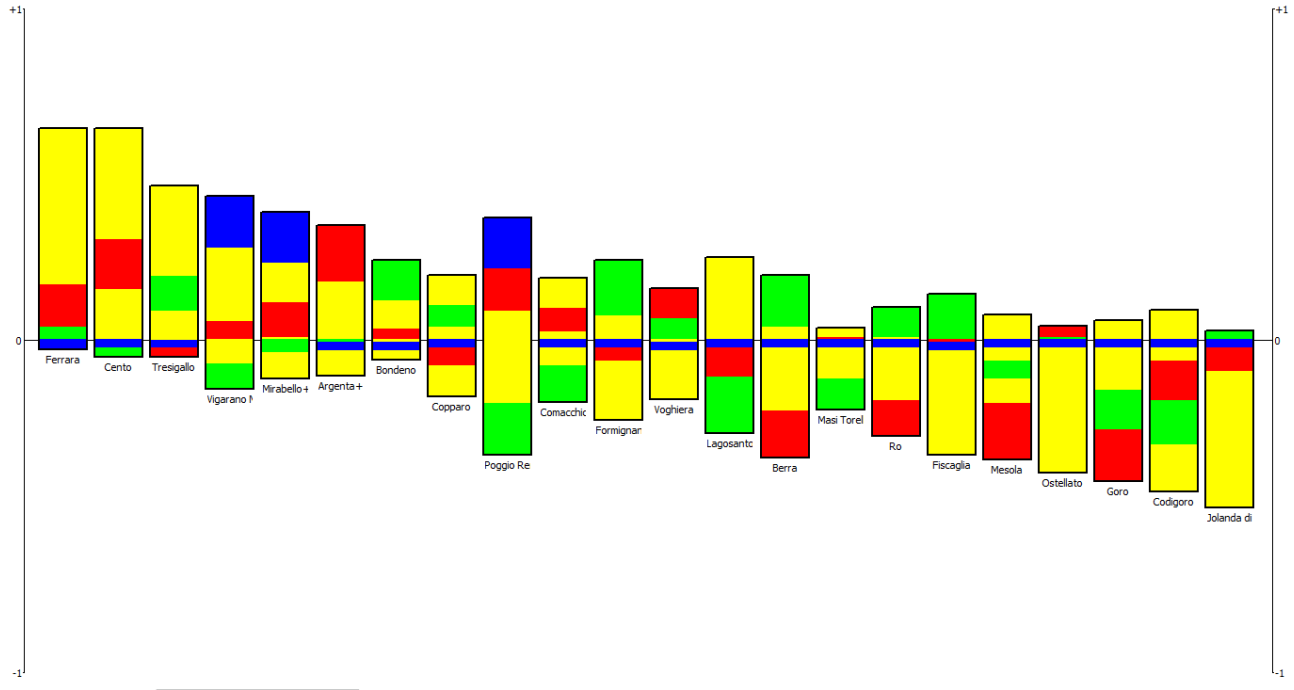

Figure 9. PROMETHEE rainbow plot for the usual preference function. On the vertical axis, the preference function Θ is reported. The yellow bar indicates the criteria relating to exposure, red is used for seismic hazard, green for vulnerability, and blue for hydraulic hazard.

Based on the ranking provided by PROMETHEE, it is possible to create a risk map of the municipalities of the province of Ferrara that highlights high-priority areas as those with a high level of combined flood and seismic risk, medium priority areas as the areas characterized by a medium combined-risk level, and, finally, low combined-risk areas.

This map is shown in Figure 10. It can be seen that the three risk levels are identified by three different colors: Red is used for high risk, orange for medium risk, and yellow for low risk.

Table 4. Ranking of alternatives for the usual preference function.

Rank	Alternatives	Θ	Θ^+	Θ^-
1	Cento	0.459	0.5086	0.0496
2	Ferrara	0.3545	0.393	0.0385
3	Tresigallo	0.1821	0.2642	0.0821
4	Mirabello + Sant'Agostino	0.1444	0.2622	0.1179
5	Argenta + Portomaggiore	0.1352	0.2182	0.0829
6	Bondeno	0.1257	0.2069	0.0812
7	Vigarano Mainarda	0.112	0.255	0.143
8	Copparo	0.0505	0.1684	0.1179
9	Poggio Renatico	0.031	0.2216	0.1906
10	Comacchio	0.0224	0.1631	0.1406
10	Voghiera	−0.0422	0.0984	0.1406
12	Formignana	−0.0721	0.0937	0.1657
13	Fiscaglia	−0.0761	0.0868	0.1628
14	Lagosanto	−0.0898	0.1385	0.2283
15	Codigoro	−0.101	0.1155	0.2164
16	Ostellato	−0.1092	0.0736	0.1828
17	Ro	−0.1362	0.0589	0.195
18	Masi Torello	−0.1371	0.0557	0.1928
19	Berra	−0.1551	0.0688	0.2239

20	Jolanda di Savoia	−0.1947	0.0408	0.2355
21	Mesola	−0.2203	0.0353	0.2556
22	Goro	−0.283	0.0137	0.2968

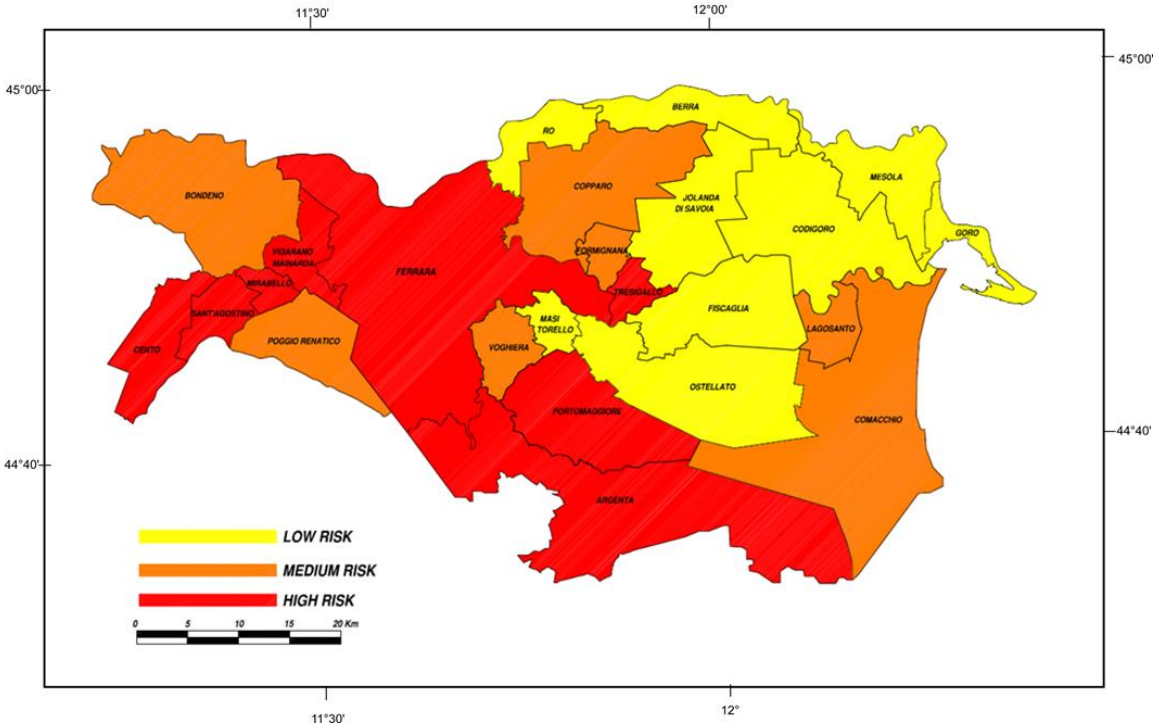

Figure 10. Multiple-risk map for the Ferrara province obtained for the usual preference function (Type 1 in Table 1). The risk levels strictly indicate the relative priority ranking for decision-makers and do not indicate the effective safety level of the various municipalities.

3.2. Linear Preference Function

The ranking of alternatives for the linear preference function and zero-max method is shown in Table 5, while the corresponding multi-risk map is shown in Figure 11. These maps were obtained by associating the quantitative criteria, i.e., flood hazard, land use, age of buildings, and population density, with a linear preference function, while thresholds q and p were determined with the zero-max method.

Table 5. Ranking of alternatives for the linear preference function and zero-max method.

Rank	Alternatives	θ	Θ^+	Θ^-
1	Cento	0.4532	0.4849	0.0317
2	Ferrara	0.3769	0.4123	0.0354
3	Tresigallo	0.2051	0.2613	0.0562
4	Vigarano Mainarda	0.1219	0.2185	0.0966
5	Mirabello+ Sant'Agostino	0.078	0.1835	0.1056
6	Lagosanto	0.0597	0.1319	0.0722
7	Poggio Renatico	0.0523	0.167	0.1147
8	Argenta+ Portomaggiore	0.0307	0.1133	0.0826
9	Copparo	0.0261	0.1107	0.0846
10	Bondeno	0.0222	0.1075	0.0853
11	Comacchio	0.0217	0.1075	0.0857
12	Codigoro	0.0125	0.1053	0.0928
13	Formignana	−0.1232	0.0146	0.1378
14	Masi Torello	−0.1275	0.0086	0.1361
15	Goro	−0.1278	0.0106	0.1384
16	Mesola	−0.1317	0.0069	0.1386
17	Berra	−0.1383	0.0046	0.1429
18	Voghiera	−0.1383	0.0041	0.1424
19	Ro	−0.1385	0.004	0.1425
20	Fiscaglia	−0.1497	0.002	0.1517

For a

21	Ostellato	−0.1839	0	0.1839
22	Jolanda di Savoia	−0.2014	0	0.2014

linear preference function of the aforementioned quantitative criteria, and thresholds q and p determined by the mean-std method, we obtained the results shown in Table 6 and Figure 12.

Table 6. Ranking of alternatives for the linear preference function and std-mean method.

By comparing the results obtained from the usual and the linear preference functions, it can be understood that changes of the preference function do not reflect large changes of the final risk maps. The only difference is that the risk levels of the municipality of Vigarano Mainarda swap with Bondeno, and Fiscaglia swaps with Lagosanto.

By comparing the maps in Figures 11 and 12, obtained with the thresholds chosen with the zero-max and mean-std methods, respectively, we observe that the risk levels of Lagosanto, Vigarano Mainarda, and Codigoro increase. Particularly, we observe that the choice of the preference function affects the final ranking of the alternatives especially when the thresholds are chosen according to the mean-std method.

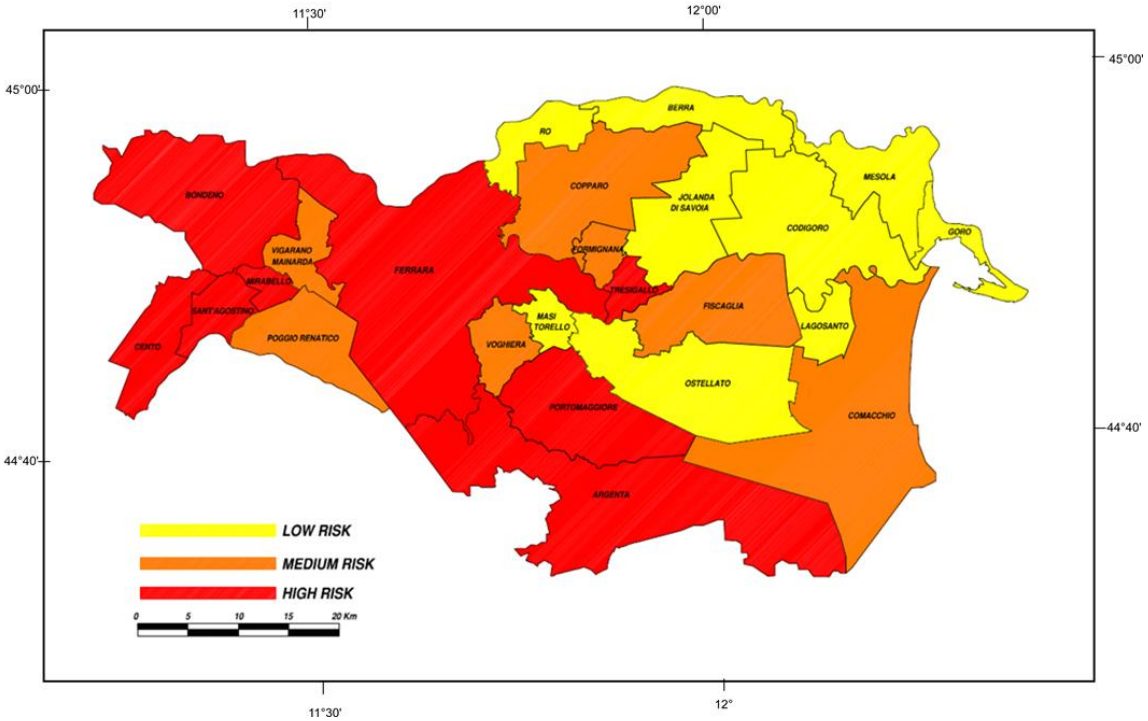

Figure 11. Multiple-risk map for the Ferrara province for the linear preference function with the thresholds chosen with the zero-max method. The risk levels strictly indicate the relative priority ranking for decision-makers and do not indicate the effective safety level of the various municipalities.

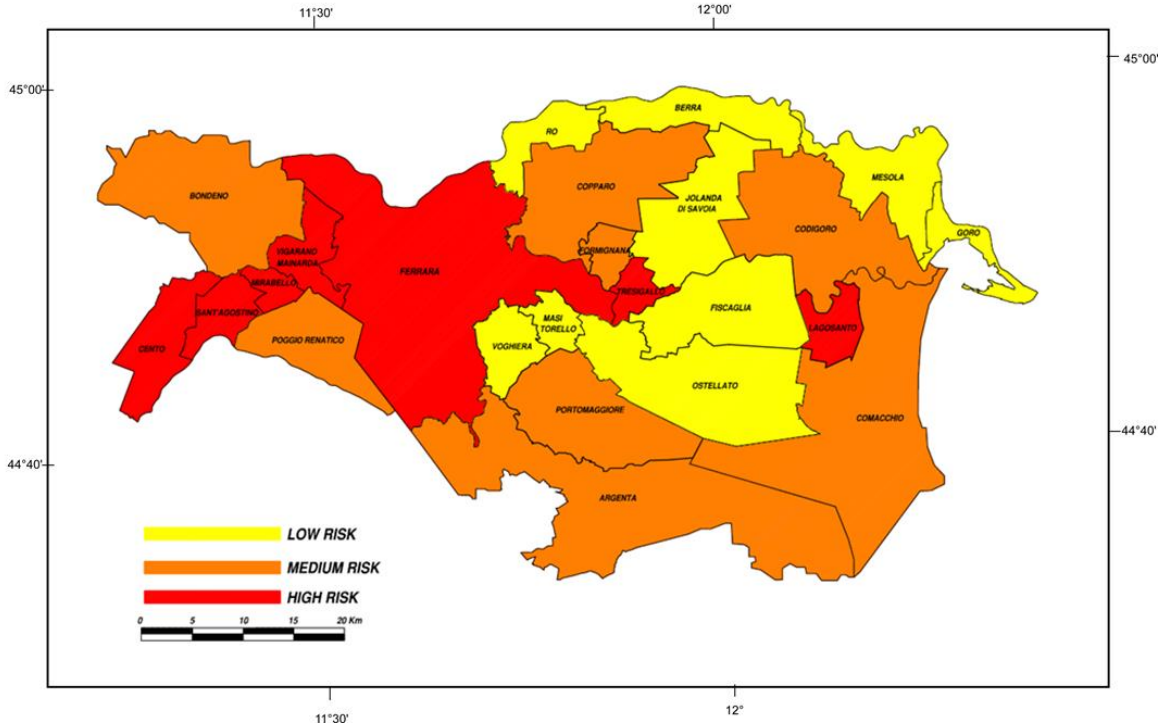

Figure 12. Multiple-risk map for the Ferrara province for the linear preference function with the thresholds chosen with the mean-std method. The risk levels strictly indicate the relative priority ranking for decision-makers and do not indicate the effective safety level of the various municipalities.

Regardless of the preference function chosen, the maps obtained present a similar risk trend, i.e., the territory is divided into two parts: The municipalities of the western part of the territory of the province of Ferrara, plus Ferrara and Tresigallo, are characterized by a medium–high risk level; the upper-eastern part of the province is characterized by a medium–low risk level.

3.3. Sensitivity Analysis on the Choice of Weights

As introduced in Section 2, the sensitivity analysis on the weights was performed by first increasing the weight of each individual criterion at a time, and then assuming the simultaneous increase in the weights of the three "exposure"-related criteria, namely land use, population density, and strategic buildings. Specifically, the weights were changed according to Scenarios 0, 1, 2, and 3 described in Table 3.

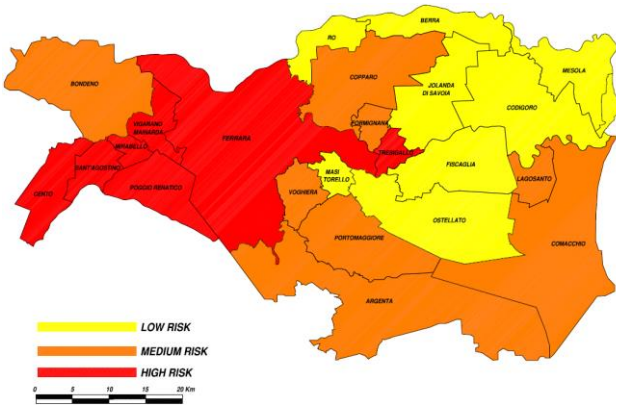
LOW RISK
MEDIUM RISK
HIGH RISK
0 5 10 15 20 Km

(a)

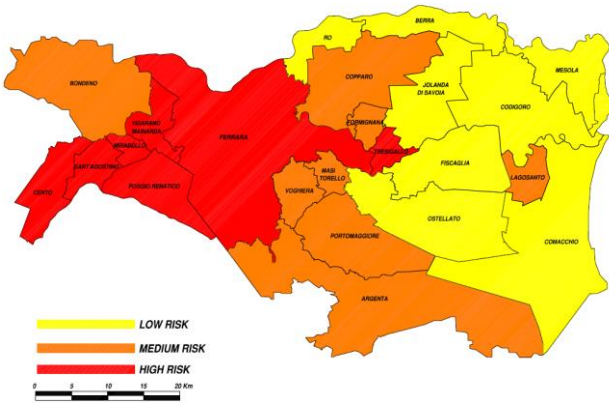
LOW RISK
MEDIUM RISK
HIGH RISK
0 5 10 15 20 Km

(b)

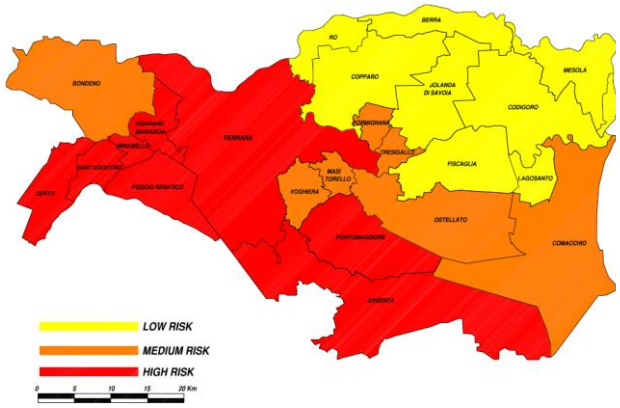
LOW RISK
MEDIUM RISK
HIGH RISK
0 5 10 15 20 Km

(c)

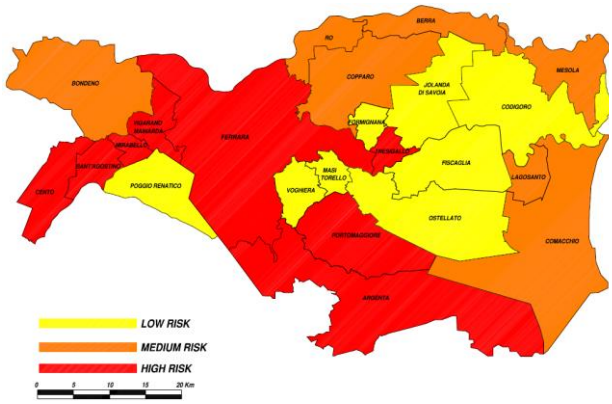
LOW RISK
MEDIUM RISK
HIGH RISK
0 5 10 15 20 Km

(d)

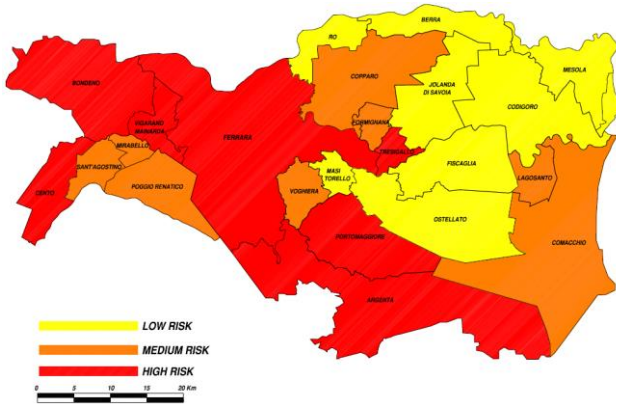
LOW RISK
MEDIUM RISK
HIGH RISK
0 5 10 15 20 Km

(e)

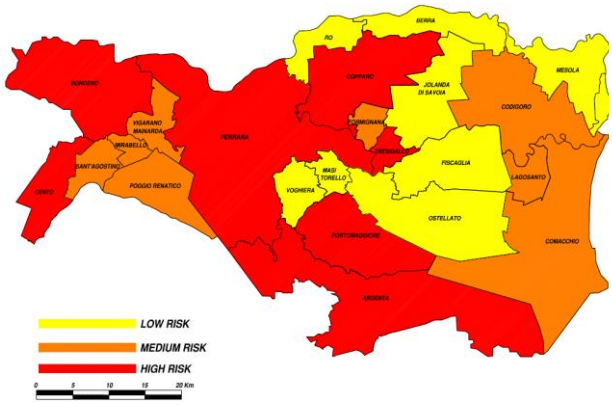
LOW RISK
MEDIUM RISK
HIGH RISK
0 5 10 15 20 Km

(f)

Figure 13. Weights sensitivity analysis, multi-risk maps; (**a**) flood hazard weight increase assuming Scenarios 2 or 3; (**b**) PGA weight increase assuming Scenario 1; (**c**) PGA weight increase assuming Scenario 2; (**d**) land use weight increase assuming Scenarios 2 or 3; (**e**) strategic buildings weight increase assuming Scenario 1; (**f**) strategic buildings weight increase assuming Scenarios 2 or 3. The risk levels strictly indicate the relative priority ranking for decision-makers and do not indicate the effective safety level of the various municipalities.

For the sake of brevity, we present hereafter the results obtained by assuming the usual preference function. For the reader's convenience, the results are reported as maps, as in the previous sections.

In the first part of the analysis, the criteria are changed according to the following order: Flood hazard, PGA, land use, strategic buildings, age of buildings, and population density. Hereafter, we omit the maps obtained for the changes of the weights relating to the criteria of strategic buildings and age of buildings, for brevity. Figures 13 and 14 illustrate the various risk maps obtained by increasing the weights.

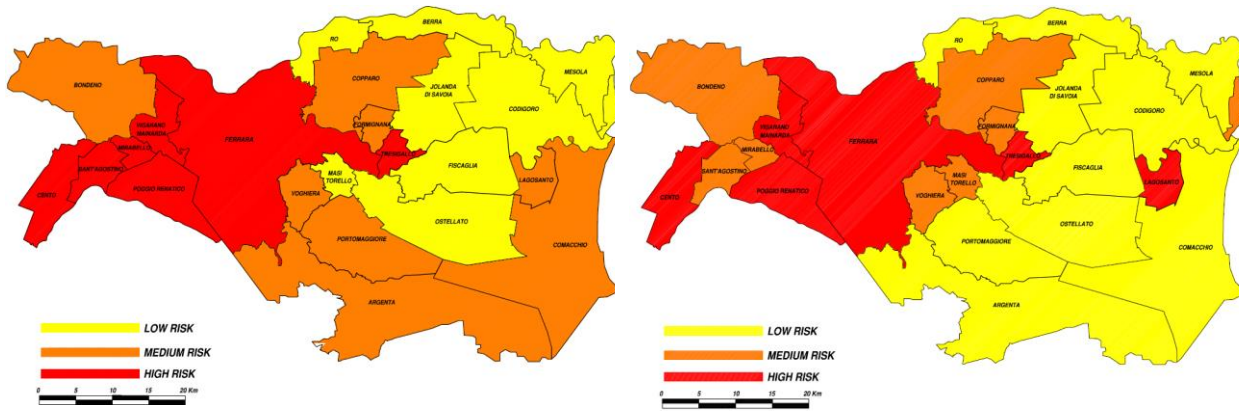

(a) (b)

Figure 14. Weights sensitivity analysis, multi-risk maps; (a) Scenario 2, population density weight increase; (b) Scenario 3, population density weight increase. The risk levels strictly indicate the relative priority ranking for decision-makers and do not indicate the effective safety level of the various municipalities.

With Scenario 1 based on the variation of the flood hazard weight, the ranking of the municipalities remains almost unchanged, as the multi-risk map is identical to that of Scenario 0. On the other

hand, the maps change when Scenarios 2 and 3 are adopted, as shown in Figure 13a. More marked differences can be observed when the weight of the PGA (Figure 13b,c) is changed. By increasing the weight of the land-use criterion, an increase in Scenario 1 does not reflect evident changes in the multi-risk map (Figure 13d). On the other hand, changes in Scenarios 2 and 3 affect the multi-risk map. Looking back at the strategic building criterion, we observe differences in the risk map when the first change of Scenario 1 is applied, compared to Scenario 0 (Figure 13e), and more so with the last two increases of Scenario 2 (Figure 13f). For the criterion of population density, the first increase in the weight according to Scenario 1 does not affect the map (see Figure 14a), while the subsequent increases in the weight bring about noticeable modifications. In particular, the multi-risk map reported in Figure 14b assigns a comparatively low level of attention to the Argenta municipality, which, however, is associated with a medium seismicity level according to the territorial classification of Figure 2a. Depending on the stakeholders' expectations, this might suggest that weights should not be varied to the extent of downgrading the seismic risk level of certain municipalities classified at medium to high seismic risk.

Lastly, results of the sensitivity on the weight choice for the criteria related to exposure are presented in Table 7. Proceeding as illustrated in Section 2, the first increase in the weight does not alter the risk map, which remains the same as in Scenario 0, whereas with the changes of Scenario 2, greater variations can be observed.

Table 7. Sensitivity analysis on the exposure factor, ranking of alternatives (EXP: EXPOSURE).

Scenario 1: WEIGHT = 0.22; OTHERS = 011					Scenario 2: WEIGHT = 0.32; OTHERS = 0.01			
Rank	Alternativa	θ	Θ^+	Θ^-	Alternativa	θ	Θ^+	Θ^-
1	Ferrara	0.7153	0.8064	0.0911	Cento	0.9452	0.9683	0.0231
2	Cento	0.7093	0.8061	0.0968	Ferrara	0.9168	0.9538	0.037
3	Tresigallo	0.5092	0.6746	0.1654	Tresigallo	0.696	0.7975	0.1015
4	Vigarano Mainarda	0.2908	0.5771	0.2863	Lagosanto	0.4603	0.6797	0.2193
5	Argenta Portomaggiore	+0.2279	0.534	0.306	Vigarano Mainarda	0.3006	0.5575	0.2569
6	Mirabello Sant'Agostino	+0.219	0.5413	0.3222	Argenta Portomaggiore	+0.2083	0.5536	0.3454
7	Bondeno	0.1597	0.4971	0.3375	Mirabello Sant'Agostino	+0.1207	0.4675	0.3468
8	Lagosanto	0.1359	0.488	0.352	Bondeno	0.1154	0.507	0.3915
9	Copparo	0.0416	0.4381	0.3965	Comacchio	0.1044	0.5017	0.3973
10	Comacchio	0.0356	0.4378	0.4022	Copparo	0.076	0.4873	0.4113
11	Poggio Renatico	−0.0499	0.4041	0.454	Mesola	−0.0919	0.3574	0.4493
12	Formignana	−0.0661	0.3555	0.4216	Masi Torello	−0.1448	0.3309	0.4757
13	Voghiera	−0.1127	0.3295	0.4422	Goro	−0.1563	0.3252	0.4815
14	Masi Torello	−0.1644	0.3064	0.4708	Codigoro	−0.1861	0.3564	0.5426
15	Berra	−0.2045	0.2863	0.4908	Poggio Renatico	−0.1924	0.3107	0.5031
16	Mesola	−0.2197	0.2787	0.4984	Formignana	−0.1938	0.3064	0.5002

17	Ro	−0.226	0.2756	0.5016	Voghiera	−0.2848	0.2607	0.5455
18	Goro	−0.2939	0.2416	0.5355	Berra	−0.2929	0.2569	0.5498
19	Codigoro	−0.3041	0.268	0.5721	Ro	−0.2949	0.2559	0.5507
20	Fiscaglia	−0.3385	0.2193	0.5578	Fiscaglia	−0.594	0.1063	0.7003
21	Ostellato	−0.4816	0.1451	0.6267	Ostellato	−0.7225	0.0418	0.7643
22	Jolanda di Savoia	−0.5829	0.0971	0.68	Jolanda di Savoia	−0.7893	0.0087	0.798

Therefore, concluding the sensitivity analysis of weights, it can be inferred that, in general, the results are sensitive to the increase in the weights of the criteria, determining a risk map that varies from case to case, causing the risk of some municipalities to decrease while that of others increased. However, these variations do not upset the overall trend, which highlights a territory divided into two parts, that of the municipalities of the western part of the territory of the province of Ferrara characterized by a medium–high risk level, and the municipalities of the north-eastern area characterized by a medium–low risk level.

3.4. Remarks on the Limitations of the Analysis

The proposed methodology requires the definition of several parameters, criteria, and weights, whose choice resulted in being strongly dependent on the expectations of stakeholders and end-users. Thus, the obtained results should be seen as a first attempt towards the proposal of an MCDA methodology that does not require great mathematical expertise, is flexible, and can be easily adapted to many situations. Nevertheless, further efforts are necessary in order for the tool to be readily exploited by public authorities and decision makers. Furthermore, it is worth highlighting other limitations inherent in the present analysis.

The first type of limitation is mainly related to the availability of data. Indeed, the choice of the criteria was based on the availability of the relevant information, which led, for some criteria, to a purely qualitative evaluation. Greater availability, accuracy, and ease of retrieval of the data would lead to the creation of a more complete and more precise analysis, and it could also contribute to the development of operational tools and software.

Secondly, this analysis neglected cascade effects, an aspect that deserves further investigation in the future [11].

Thirdly, the present contribution does not consider the impact of modeling assumptions on the seismic risk assessment. At the relevant scale of observations of the present analysis, specific structural aspects connected to the vulnerability levels of the buildings cannot be easily considered. In this regard, we recall that specific structural aspects and modeling assumptions play, among others, a key role for seismic risk evaluation at both the building and the urban scale [36]. A recent study focusing on South America has shown the uncertainties and biases that the use of simplified models or heterogenous data may produce in the determination of seismic vulnerability [36]. For completeness, seismic risk evaluation is extensively discussed, for instance, in the aforementioned contributions [36–39] and the references cited therein.

Finally, we recall that the seismic classification shown in Figure 2 has been merely used as a technical-administrative reference for establishing the priority of actions and measures aimed at preventing and mitigating seismic risk. It must not be used to determine the local seismic action or for the structural design of buildings, which, instead, rely upon more detailed maps highlighting, for instance, the presence of site effects due to the inherent geological structure of the ground or instability effects such as liquefaction. Therefore, the present analysis should be purposefully extended in order to consider the aforementioned local effects [40].

B.4. Conclusions

For the present case study, the application of the Multiple-Criteria Decision Analysis (MCDA) methodology through the PROMETHEE algorithm has proved an innovative and promising operational tool. Its potential derives from the ability to both analyze information from various sources and jointly systematize data expressed in different units and scales. The application of this methodology has made it possible to rank the various municipalities in terms of the relative proneness to joint flood and seismic hazards. We recall that the objective of the methodology is not to quantify the safety level in absolute terms of the various municipalities. Its scope is, indeed, to provide useful information for decision makers and public authorities to define future intervention priorities. We further emphasize that, in the authors'opinion, the present study is original as it applies the PROMETHEE algorithm for the first time to a multi-risk assessment of seismic and flood hazards.

Depending on the territory to be studied, the relevant risks could be different, and therefore, different criteria must be used to express them. Nevertheless, the generalization to other multi-risk analyses and different case studies deserves further considerable efforts and thoughtful insights. Full validation of the present methodology is also of utmost importance and calls for new

developments. However, the proposed methodology is flexible. This suggests that, with due precautions and adaptations, it is possible to apply it to different risk scenarios, such as scenarios including coastal floods and landslides, while keeping the same applicative scheme.

Finally, the obtained results have shown that the proposed methodology is an operational tool that, once further validated, can be used by end users, whether modelers or decision makers, to urgently allocate resources and increase the coping capacity of communities in the case of catastrophic events.

B. References

1. UN-ISDR. Sendai Framework for Disaster Risk Reduction 2015–2030. In Proceedings of the UN world Conference on Disaster Risk Reduction, 14–18 March 2015, Sendai, Japan; United Nations Office for Disaster Risk Reduction: Geneva, Switzerland. Available online: http://www.unisdr.org/files/43291_sendaiframeworkfordrren.pdf (accessed on 1 October 2021).

2. Poljanšek, K.; Ferrer, M.M.; De Groeve, T.; Clark, I. Preface. In: *Science for Disaster Risk Management 2017: Knowing Better and Losing Less*; Publications Office of the European Union: Luxembourg, 2017; ISBN 978-92-79-60678-6. https://doi.org/10.2788/688605, JRC102482.

3. Topics Geo: Natural Catastrophes 2013: Analyses, Assessments, Positions, Münchener Rückversicherungs-Gesellschaft, Munich, 2014. Available online: https://www.munichre.com/content/dam/munichre/contentlounge/website-pieces/documents/302-08121_en.pdf/_jcr_content/renditions/original./302-08121_en.pdf (accessed on).

4. UN-ISDR. Terminology: Basic Terms of Disaster Risk Reduction. 2009. Available online: http://www.unisdr.org./we/inform/terminology (accessed on 1 October 2021).

5. Urlainis, A.; Ornai, D.; Levy, R.; Vilnay, O.; Shohet, I.M. Loss and damage assessment in critical infrastructures due to extreme events. *Saf. Sci.* 2022, *147*, 105587.

6. Kanamori, H.; Hauksson, E.; Heaton, T. Real-time seismology and earthquake hazard mitigation. *Nature*, 1997, *390*, 461–464.

7. Quesada-Román, A.; Villalobos-Chacón, A. Flash flood impacts of Hurricane Otto and hydrometeorological risk mapping in Costa Rica. *Geogr. Tidsskr. -Dan. J. Geogr.* 2020, *120*, 142–155.

8. Quesada-Román, A.; Ballesteros-Cánovas, J.A.; Granados-Bolaños, S.; Birkel, C.; Stoffel, M. Improving regional flood risk assessment using flood frequency and dendrogeomorphic analyses in mountain catchments impacted by tropical cyclones. *Geomorphology* 2022, *396*, 108000.

9. Kron, W. Reasons for the increase in natural catastrophes: The development of exposed areas. In *Topics 2000: Natural Catastrophes, the Current Position*; Munich Reinsurance Company, Munich, Germany, 1999; pp. 82–94.

10. Barredo, J. I. Major flood disasters in Europe: 1950–2005. *Nat. Hazards* 2007, *42*, 125–148.

11. Zuccaro, G.; De Gregorio, D.; Leone, M.; Theoretical model for cascading effects analyses. *Int. J. Disaster Risk Reduct.* 2018, *30*, 199–215.

12. Zschau, J. Where are we with multihazards, multirisks assessment capacities? In *Science for Disaster Risk Management 2017: Knowing Better and Losing Less*; Poljansek, K.; Marin Ferrer, M.; De Groeve, T., Eds.; Publications Office of the European Union: Luxembourg, 2017; ISBN 978-92-79-60678-6. https://doi.org/10.2788/688605, JRC102482.

13. Fuchs, S.; Keiler, M.; Zischg, A. A spatiotemporal multi-hazard exposure assessment based on property data. *Nat. Hazard. Earth Syst. Sci.* 2015, *15*, 2127–2142.

14. Komentova, N.; Scolobig, A.; Garcia-Aristizabal, A.; Monfort, D.; Fleming, K. Multi-risk approach and urban resilience. *Int. J. Disast. Res. Built Env.* 2016, 7, 114–132.

15. Marzocchi, W.; Garcia-Aristizabal, A.; Gasparini, P.; Mastellone, M.L.; Di Ruocco, A. Basic principles of multi-risk assessment: A case study in Italy. *Nat. Hazards* 2012, *62*, 551–573.

16. Kappes, M.S.; Keiler, M.; von Elverfeldt, K.; Glade, T. Challenges of analyzing multi-hazard risk: A review. *Nat. Hazards* 2012, *64*, 1925–1958.

17. Bell, R.; Glade, T. Multi-hazard analysis in natural risk assessments. *WIT Trans. Ecol. Environ.*, 2004, *77*, 1–10.

18. Schmidt, J.; Matcham, I.; Reese, S.; King, A.; Bell, R.; Henderson, R.; Smart, G.; Cousins, J.; Smith, W.; Heron, D. Quantitative multi-risk analysis for natural hazards: A framework for multi-risk modelling. *Nat. Hazards* 2011, *58*, 1169–1192.

19. Neri, A.; Aspinall, W.P.; Cioni, R.; Bertagnini, A.; Baxter, P.J.; Zuccaro, G.; Andronico, D.; Barsotti, S.; Cole, P.D.; Esposti Ongaro, T.; et al. Developing an Event Tree for probabilistic hazard and risk assessment at Vesuvius. *J. Volcanol. Geoth. Res*. 2008, *178*, 397–415.

20. Barthel, F.; Neumayer, E. A trend analysis of normalized insured damage from natural disasters. *Clim. Chang.* 2012, *113*, 215–237.

21. Skilodimou, H.D.; Bathrellos, G.D.; Chousianitis, K.; Youssef, A.M.; Pradhan, B. Multi-hazard assessment modeling via multi-criteria analysis and GIS: A case study. *Envir. Earth Sci*. 2019, *78*, 47.

22. Brans, J.P.; Mareschal, B. Promethee Methods. In M*ultiple Criteria Decision Analysis: State of the Art Surveys*; Figueira, J., Greco, S., Ehrogott, M., Eds.; Springer: Berlin/Heidelberg, Germany, 2005.

23. Gallina, V.; Torresan, S.; Critto, A.; Sperotto, A.; Glade, T.; Marcomini, A. A review of multi-risk methodologies for natural hazards: Consequences and challenges for a climate change impact assessment. *J. Environ. Manag.* 2016, *168*, 123–132.

24. Gallina, V.; Torresan, S.; Zabeo, A.; Critto, A.; Glade, T.; Marcomini, A. A Multi-Risk Methodology for the Assessment of Climate Change Impacts in Coastal Zones. *Sustainability* 2020, *12*, 3697.

25. Peduzzi, P.; Dao, H.; Herold, C.; Mouton, F. Assessing global exposure and vulnerability towards natural hazards: The Disaster Risk Index, *Nat. Hazards Earth Syst. Sci*. 2009, *9*, 1149–1159.

26. Brans, J.P.; Vincke, Ph.; Mareschal, B. How to select and how to rank projects: The PROMETHEE method. *Eur. J. Oper. Res*. 1986, *24*, 228–238.

27. Mladineo, M.; Jajac, N.; Rogulj, K.; A simplified approach to the PROMETHEE method for priority setting in management of mine action projects, *Croat. Oper. Res. Rev*. 2016, *7*, 249–268.

28. Crnjac, M.; Aljinovic, A.; Gjeldum, N.; Mladineo, M. Two-stage product design selection by using PROMETHEE and Taguchi method: A case study. *Adv. Prod. Eng. Manag.* 2019, *14*, 39–50.

29. Savic, M.; Nikolic, D.; Mihajlovic, I.; Zivkovic, Z.; Bojanov, B.; Djordjevic, P. Multi-Criteria Decision Support System for Optimal Blending Process in Zinc Production. *Miner. Processing Extr. Metall. Rev.* 2015, *36*, 267–280.

30. Rocchi, A.; Chiozzi, A.; Nale, M.; Nikolic, Z.; Riguzzi, F.; Mantovan, L.; Gilli, A.; Benvenuti, E. A Machine Learning Framework for Multi-Hazard Risk Assessment at the Regional Scale in Earthquake and Flood-Prone Areas. *Appl. Sci.* 2022, *12*, 583.

31. Carminati, E.; Martinelli, G. Subsidence rates in the Po Plain, northern Italy: The relative impact of natural and anthropogenic causation. *Engng. Geol.* 2002, *66*, 241–255.

32. Salvati, L.; Mavrakis, A.; Colantoni, A.; Mancino, G.; Ferrara, A. Complex Adaptive Systems, soil degradation and land sensitivity to desertification: A multivariate assessment of Italian agro-forest landscape. *Sci. Total Env.* 2015, *521–522*, 235–245.

33. Stucchi, M.; Meletti, C.; Montaldo, V.; Akinci, A.; Faccioli, E.; Gasperini, P.; Malagnini, L.; Valensise, G. Pericolosità Sismica di Riferimento Per il Territorio Nazionale MPS04 [Data set]. Istituto Nazionale di Geofisica e Vulcanologia (INGV). 2004. Available online: https://doi.org/10.13127/sh/mps04/ag (accessed on 1 October 2021).

34. Trigila, A.; Iadanza, C.; Bussettini, M.; Lastoria, B. *Dissesto Idrogeologico in Italia: Pericolosità e Indicatori di Rischio—Edizione 2018*; Rapporti 287/2018; ISPRA: Roma, Italy, 2018.

35. Decreto Legislativo n. 49/2010. Available online: https://www.mite.gov.it/sites/default/files/archivio/allegati/vari/documento_definitivo_indirizzi_operativi_direttiva_alluvioni_gen_13.pdf (accessed on 3 January 2022).

36. Dolce, M.; Prota, A.; Borzi, B.; da Porto, F.; Lagomarsino, S.; Magenes, G.; Moroni, C.; Penna, A.; Polese, M.; Speranza, E.; Verderame, G.M. Seismic risk assessment of residential buildings in Italy. *Bull. Earthquake Eng.* 2021, *19*, 2999–3032. https://doi.org/10.1007/s10518-020-01009-5.

37. Hoyos, M.C.; Hernández, A.F. Impact of vulnerability assumptions and input parameters in urban seismic risk assessment. *Bull. Earthquake Eng.* 2021, *19*, 4407–4434.

38. Asadi, E.; Salman, A.M.; Li, Y.; Yu, X. Localized health monitoring for seismic resilience quantification and safety evaluation of smart structures. *Struct. Saf.* 2021, *93*, 102127.

39. Joyner, M.D.; Gardner, C.; Puentes, B.; Sasani, M. Resilience-Based seismic design of buildings through multiobjective optimization. *Eng. Struct.* 2021, *246*, 113024.

40. CTMS. 2015: Linee guida per la gestione del territorio in aree interessate da Faglie Attive e Capaci (FAC). Commissione tecnica per la microzonazione sismica, Gruppo di lavoro FAC. Dipartimento della Protezione Civile e Conferenza delle Regioni e delle Province Autonome. Available online: http://www.protezionecivile.gov.it/resources/cms/documents/LineeGuidaFAC_v1_0.pdf (accessed on 3 January 2022).